International Journal of Thermophysics (2026) 47:32
https://doi.org/10.1007/s10765-025-03682-7

Alcohol–Additive Ternary Mixtures for Sustainable Fuel Formulations: Experimental Excess Molar Enthalpy and Thermodynamic Modeling

Fatima Ezzahra Yatim[1] · Khaoula Samadi[1,2] · Mohamed Lifi[3] · Fernando Aguilar[2] · Fatima Ezzahrae M.'hamdi Alaoui[1]

Received: 15 September 2025 / Accepted: 8 November 2025 / Published online: 13 January 2026

Abstract

Fuel blends incorporating oxygenated additives are increasingly explored to enhance combustion efficiency and reduce greenhouse gas emissions. Understanding the thermodynamic behavior of such mixtures is essential for optimizing their formulation. In this study, the excess molar enthalpy (H_m^E) a key property reflecting molecular interactions and non-ideality was measured for four ternary blends containing 2-(2-methoxyethoxy)ethanol, 2-(2-ethoxyethoxy)ethanol, 2-methoxyethanol, and 2-phenoxyethanol, each mixed with ethanol, at 298.15 and 313.15 K under 0.1 MPa using a quasi-isothermal flow calorimeter. The experimental results were correlated using the Redlich–Kister, NRTL, and UNIQUAC models, while the predictive performance of the Modified UNIFAC (Dortmund) model was also assessed. Positive H_m^E values were obtained for all mixtures, indicating endothermic mixing and dominant dispersive–dipolar interactions. Among the applied models, the Redlich–Kister equation provided the best correlation with experimental data. The results contribute valuable thermodynamic benchmarks for modeling the energetics of oxygenated fuel blends and improving predictive approaches for complex liquid mixtures.

Keywords Excess Molar Enthalpy · Ternary mixtures · Oxygenated additives · Redlich–Kister correlation · Local composition Models · Modified UNIFAC (Dortmund) model

✉ Mohamed Lifi
mlifi@ubu.es

[1] Energy Laboratory, Faculty of Sciences, University of Abdelmalek Essaadi, Tetouan, Morocco

[2] Departamento de Ingeniería Electromecánica, Escuela Politécnica Superior, Universidad de Burgos, 09006 Burgos, Spain

[3] Department of Mathematics and Computing, Faculty of Science, University of Burgos, 09001 Burgos, Spain

1 Introduction

In recent years, the development of combustion engine technologies has attracted significant research attention [1]. In this context, new concepts have emerged, among which fuel design strategies play an important role. This approach signifies the optimal combination of different fuels to enhance both physical and chemical properties, with the main objective of achieving high combustion efficiency while simultaneously reducing emissions.

Global fossil fuel reserves are continuously decreasing. Additionally, fossil-fuel-based engines contribute substantially to environmental pollution, particularly through the emission of nitrogen oxides and particulate matter. However, growing demand remains high in the industrial and transport sectors, primarily due to their high energy density and economic competitiveness compared with eco-friendly alternatives.

Nowadays, alternative fuels such as alcohols, glycol ethers and biodiesel are increasingly promoted, especially in the transport sector [2], because of their contribution to a secure, sustainable, and affordable energy future [3]. However, the complete substitution of fossil fuels with alternatives remains a challenge. Consequently, blending conventional fuels (diesel and gasoline) with oxygenated additives has emerged as a promising solution [1, 4]. Furthermore, In addition, synthesizing new additives by combining different oxygenated compounds has shown excellent results, including improved miscibility and significant reductions in emissions [5]. The oxygen content of these additives enhances combustion by promoting complete oxidation, thereby improving overall efficiency [1, 6]. For example, in a ternary blend of diesel, vegetable oil, and diethyl ether tested in a compression ignition engine [7], performance levels comparable to pure diesel were achieved using a mixture containing only 60% diesel. Furthermore, improved combustion efficiency and a remarkable 77% reduction in pollutant emissions were observed [8].

Alcohols such as ethanol and 1-butanol offer several advantages, including favorable burning properties, easy handling and storage and cost-effectiveness, [9]. Both ethanol and 1-butanol are produced through biomass fermentation and are therefore considered renewable energy sources. As additives, n-butanol has been shown to improve both performance and emissions, whereas ethanol has demonstrated improvements primarily in emissions [4]. Furthermore, 1-butanol possesses a higher energy content and better miscibility compared to ethanol. I Despite these advantages, the direct use of ethanol or 1-butanol in pure form is limited by technical and economic constraints [7]. Pure usage would require substantial engine modifications or the addition of specialized additives to optimize lubrication and ignition properties [6]. Engine modifications are generally not considered an optimal solution, while the use of tailored additives appears more favorable. Notably, 1-butanol can also be synthesized via propylene hydroformylation, giving it both petrochemical and industrial origins. Similarly, 2-(2-methoxyethoxy)ethanol, 2-(2-ethoxyethoxy)ethanol, 2-methoxyethanol, and 2-phenoxyethanol are synthetic glycol ethers that can serve as suitable fuel additives. Their molecular structure, which combines ether and hydroxyl functional groups, provides excellent solvency for both polar

and non-polar substances. Consequently, their main role in fuel blends is to enhance miscibility, stability, and combustion performance [10].

Excess molar enthalpy is a thermos-physical property of fuels that is strongly affected by variations in temperature and pressure. To accurately simulate real fuel applications, it is essential to investigate this property under operating conditions representative of the transport and industrial sectors.

For temperature, $T = 298.15$ K is widely recognized as the standard reference for thermodynamic measurements. It corresponds to ambient conditions and represents the typical temperature at which fuels enter engines, as well as the conditions relevant for handling, blending, and storage [11]. Measurements at 298.15 K are also essential for comparison with literature data, enabling consistency across studies and providing reliable input for engineering databases and process simulation tools [12]. In addition, $T = 313.15$ K is frequently used to approximate the fuel temperature inside injectors and pipelines during engine operation. This temperature is also relevant for a variety of chemical and separation processes such as liquid–liquid extraction, distillation, and biodiesel purification that are typically carried out between 30 and 60 °C. Thus, experimental data at 313.15 K contribute to the optimization of both fuel systems and industrial processes [13, 14]. Along with atmospheric pressure ($p = 0.1$ MPa), these two reference temperatures 298.15 K and 313.15 K, have crucial importance for determining and modeling the thermos-physical properties of fuels [13, 15, 16].

In this work, four ternary mixtures were prepared: x_1 2-(2-methoxyethoxy) ethanol + x_2 1-butanol + (1-x_1-x_2) ethanol, x_1 2-(2-ethoxyethoxy)ethanol + x_2 1-butanol + (1-x_1-x_2) ethanol, x_1 2-methoxyethanol + x_2 1-butanol + (1-x_1-x_2) ethanol, x_1 2-phenoxyethanol + x_2 1-butanol + (1-x_1-x_2) ethanol. The excess molar enthalpies of these blends were measured at $T = (298.15$ and $313.15)$ K and $p = 0.1$ MPa using a quasi-isothermal flow calorimeter. The experimental data were then fitted using the Redlich Kister equation [17], and predicted with NRTL [18], UNIQUAC [19] and modified UNIFAC (Dortmund) [20] models.

2 Chemicals

The components investigated in this study are 2-(2-methoxyethoxy)ethanol (22MEE) ($C_5H_{12}O_3$); 2-(2-ethoxyethoxy)ethanol (22EEE) ($C_6H_{14}O_3$); 2-methoxyethanol (2ME) ($C_3H_8O_2$); 2-phenoxyethanol (2-PhE) ($C_8H_{10}O_2$); 1-butanol (1-BuOH) ($C_4H_{10}O_2$); and ethanol (C_2H_6O). These compounds were used to prepare four ternary mixtures in which each glycol ether (22MEE, 22EEE, 2ME, or 2-PhE) was combined with 1-BuOH and ethanol. Relevant physicochemical data of the pure substances, including molecular formula, molar mass, density, mole fraction purity, water content, and CAS number, are listed in Table 1. All chemicals were supplied with a mass fraction purity higher than 99%, and no further purification was required prior to use. The initial water contents of the solvents, as provided by the supplier, were determined by Karl-Fischer coulometric titration (Mettler Toledo C20 coulometric titrator, sensitivity 0.1 µg H_2O) in accordance with ASTM E203 and ISO 760 standards. After sample handling, the water content of all components was reverified

Table 1 Purity and chemical data of used liquids

Compound	Formula	Molar mass (g/mol)	Density (g/cm^3)				State mole fraction purity[2]	Water content (mass %)[3]	CAS number
			Experiment[1]		Literature				
			298.15 K	313.15 K	298.15 K	313.15 K			
22MEE*	$C_5H_{12}O_3$	120.15	1.0147	1.0014	1.0154[a]	1.0020[b]	> 99.0	≤ 0.03	111–77-3
22EEE*	$C_6H_{14}O_3$	134.18	0.9852	0.9718	0.9843[c]	0.9709[c]	> 99.0	≤ 0.03	111–90-0
2ME*	$C_3H_8O_2$	76.09	0.9598	0.9460	0.9601[d]	0.9459[e]	> 99.8	≤ 0.01	109–86-4
2-PhE*	$C_8H_{10}O_2$	138.18	1.1030	1.0900	1.1034[f]	1.0830[g]	> 99.0	≤ 0.02	122–99-6
1-BuOH*	$C_4H_{10}O$	74.12	0.8055	0.7941	0.8060[h]	0.7943[i]	> 99.5	≤ 0.02	71–36–3
Ethanol	C_2H_6O	46.07	0.7852	0.7718	0.7849[j]	0.7721[j]	> 99.8	≤ 0.03	64–17-5

[a]belhadj et al. [21]; [b]Mozo et al. [22]; [c]Francesconi et al. [23]; [d]Holgado et al. [24]; [e]Reghem et al. [25]; [f]Alonso et al. [26]; [g]Rana et al. [27]; [h]Yang et al. [28]; [i]Valles et al. [29]; [j]Pandharinath et al. [30]

[1]Densities have been measured using a vibrating-tube densimeter (Anton Paar DSA 5000 M). Calibration was performed with air and doubly distilled water as reference fluids before each measurement series. The combined expanded uncertainty of the density values is estimated to be 0.003 g·cm^{-3}

[2]Determined by gas chromatography (GC) by the supplier

[3]Water content determined by Karl–Fischer coulometric titration (Mettler Toledo C20 coulometric titrator, sensitivity 0.1 µg H_2O)

*22MEE: 2-(2-Methoxyethoxy)ethanol; 22EEE: 2-(2-Ethoxyethoxy)ethanol; 2ME: 2-Methoxyethanol; 2-PhE: 2-Phenoxyethanol; 1-BuOH: 1-Butanol

using the same Karl-Fischer coulometric method. For the four alkoxyethanols, no change was detected; the samples were taken directly from their designated storage bottles, ensuring the purity of the substances and preventing any possibility of water absorption prior to use. For ethanol, the new measured value was ≤ 0.03 mass %, while for 1-butanol no change was observed. The slight variation in ethanol is attributed to its hygroscopic nature and to the preparation of four fractions between these two components for each ternary mixture. Moreover, the low boiling point of ethanol facilitates minor water absorption during handling.

3 Materials & Methods

A quasi-isothermal calorimeter was employed to determine the H_m^E of the investigated binary and ternary mixtures. A schematic representation of the experimental setup is given in Fig. 1. Experiments were carried out at 298.15 and 313.15 K. The mole fractions (x_i) of the mixture components were obtained from the measured flow rates of the liquids, together with their molecular weights and densities. The associated standard uncertainty was estimated as $u(x) = 0.0008$. Table 1 reports the densities, ρ, of the measured pure compounds at the delivery temperatures, which are also compared with literature data [21–30]. Densities (ρ) of the pure compounds

were measured at the delivery temperatures using a vibrating-tube densimeter (Anton Paar DSA 5000 M). Calibration was performed with air and doubly distilled water as reference fluids before each measurement series. The combined expanded uncertainty of the density values is estimated to be 0.003 g·cm^{-3}. The dependence of H_m^E on composition was studied by preparing mixtures of different mole fractions. The excess molar enthalpy was obtained from the relation:

$$H_m^E = \frac{Q_{mixture}}{\dot{n}_{mixture}}, \tag{1}$$

where $Q_{mixture}$ is the measured heat effect of mixing, and $\dot{n}_{mixture}$ is the total molar flow rate of the solution. Thus, H_m^E for each composition was determined by dividing the thermal power released in the mixing cell by the molar flow rate of the mixture. In binary systems, both streams correspond to the pure liquids, whereas in ternary mixtures one stream is a pure liquid and the other was a pre-mixed binary solution. The expanded relative uncertainty associated with the excess molar enthalpy measurements was evaluated as ($k=2$) Ur (H_m^E) = 1%. An in-depth explanation and validation of the experimental procedure can be found in our earlier work [31]. The uncertainty budget of H_m^E, calculated following the EA-4/02 guidelines [32], is summarized in Table 2.

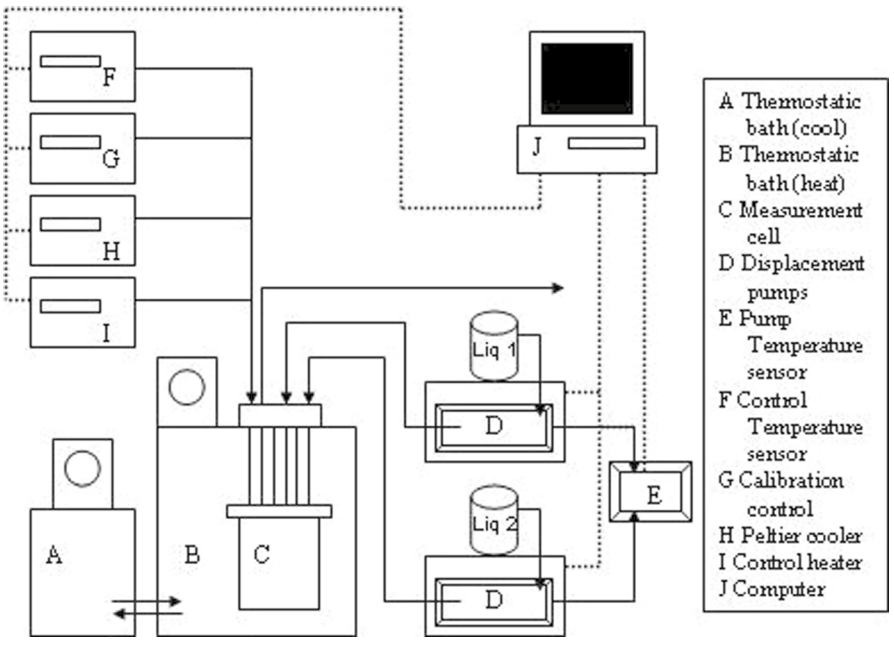

Fig. 1 Quasi-isothermal flow calorimeter. Schematic diagram

4 Equations and Models

The R–K, NRTL, and UNIQUAC models were used in this work as correlative models, in which the binary interaction parameters were optimized to reproduce the experimental excess molar enthalpies. In contrast, the Modified UNIFAC (Dortmund) model was applied as a predictive model, where all group interaction parameters were taken directly from the literature without any adjustment to the experimental data. This distinction highlights that the first three models rely on regression to fit the data, whereas UNIFAC-DMD provides independent predictions based on the group-contribution approach.

4.1 Modified Redlich–Kister Equation

Binary mixture results were analyzed using the R-K equation [17], expressed as:

$$H_m^E = \frac{x(1-x)\sum_{i-1}^{n} A_i(2x-1)^{i-1}}{1+A_0(2x-1)}, \tag{2}$$

where A_i coefficients were obtained by the unweighted least-squares method. The optimal number of coefficients was determined using the F-test [33].

4.2 NRTL Model

Excess molar enthalpies were also correlated using the Non-Random Two-Liquid (NRTL) model [18]. The general expression is given by:

$$H_m^E = -RT\sum_{i=1}^{n} x_i\eta_i, \tag{3}$$

Table 2 Uncertainty budget for excess enthalpy using EA-4/02 [32].*

		Units	Estimate	Divisor	uncertainty value
$U(Q_{mixture})$	Resolution	W	$4{\cdot}10^{-6}$	$2\sqrt{3}$	$1.15{\cdot}10^{-6}$
$u(Q_{mixture})$	Repeatability		$4{\cdot}10^{-6}$	1	$4{\cdot}10^{-6}$
$u(Q_{mixture})$	Non-linearity		$1.2{\cdot}10^{-4}$	1	$1.2{\cdot}10^{-4}$
$U(\dot{V}_1)$	Accuracy	$cm^3{\cdot}s^{-1}$	$2.5{\cdot}10^{-5}$	2	$1.25{\cdot}10^{-5}$
	Resolution		$1.7{\cdot}10^{-5}$	$2\sqrt{3}$	$7.22{\cdot}10^{-6}$
$U(\dot{V}_2)$	Accuracy	$cm^3{\cdot}s^{-1}$	$2.5{\cdot}10^{-5}$	2	$1.25{\cdot}10^{-5}$
	Resolution		$1.7{\cdot}10^{-5}$	$2\sqrt{3}$	$7.22{\cdot}10^{-6}$
$u(T)$	Stability	K	$1{\cdot}10^{-2}$	1	0.01
$u(H_m^E)$	$H_m^E = 400$	$J{\cdot}mol^{-1}$	N/A	$k=1$	0.9
$U(H_m^E)$		$J{\cdot}mol^{-1}$	N/A	$k=2$	1.8
$U_r(H_m^E)$		$J{\cdot}mol^{-1}/J{\cdot}mol^{-1}$	N/A	$k=2$	$5{\cdot}10^{-3}$

*$Q_{mixture}$: heat of mixing; $\dot{V}_1$ and $\dot{V}_2$: flows of pure components 1 and 2 driven by isocratic pumps; T: temperature; H_m^E: excess enthalpy; x: mole fraction

where x_i is the fractional composition of compound i and η_i is is defined as:

$$\eta_i = \frac{\sum_{k=1}^{p} x_k \tau_{ki} G_{ki} \left[\alpha\left(\tau_{ki} - \left(\sum_{n=1}^{p} x_n \tau_n G_n / \sum_{l=1}^{n} x_l G_{li}\right)\right) - 1\right]}{\sum_{l=1}^{n} x_l G_{li}} \tag{4}$$

α accounts for non-uniformity of molecular forces, thereby enhancing the accuracy of phase equilibrium predictions. In the NRTL framework, G_{ji} is expressed as $G_{ji} = exp\ (-\ \alpha\tau_{ij})$, where $\tau_{ij} = (g_{ij} — g_{ii})/RT$, with g_{ij} representing the strength of intermolecular forces expressed as interaction energy between i and j. The NRTL model is particularly well-suited for systems dominated by strong hydrogen bonding.

4.3 Uniquac Model

The UNIQUAC model [19] was employed to describe the correlation of the excess molar enthalpies, H_m^E. Its mathematical form is given as:

$$H_m^E = \sum_{i=1}^{n} q_i x_i \frac{\sum_{j=1}^{n} \vartheta_j \Delta u_{ji} \tau_{ji}}{\sum_{j=1}^{n} \vartheta_j \tau_{ij}}, \tag{5}$$

where $\vartheta_j = \frac{q_i x_i}{\sum_j q_i x_i}$ and q_i represents the molecular surface area, obtained by adding the contributions of the functional groups present in the molecule.

4.4 Modified UNIFAC (Dortmund) Model

UNIFAC model [20, 34], an extension of UNIQUAC based on group contributions, was employed to predict activity coefficients. The corresponding equation is:

$$H_m^E = -RT^2 \sum_i \sum_k x_i v_K^{(i)} \left[\left(\frac{\partial ln \Gamma_K}{\partial T} \right)_{p,x} - \left(\frac{\partial ln \Gamma_K^{(i)}}{\partial T} \right)_{p,x} \right] \tag{6}$$

$v_K^{(i)}$ is the number of groups of type k in molecule i. R is the universal gas constant, and T is the absolute temperature.

4.5 Accuracy Test

To evaluate the accuracy of the correlations, the following statistical metrics were employed: Absolute Average Deviation (AAD), Root Mean Square (RMS), maximum deviation (max ($|H_m^E|$)).

$$AAD = \frac{100}{N} \sum_{i=1}^{N} \left| \frac{H_{m,exp}^E - H_{m,calc}^E}{H_{exp}^E} \right| \tag{7}$$

$$RMS = \left[\frac{\sum_{i=1}^{N} \left(H^{E}_{m,exp} - H^{E}_{m,calc} \right)^{2}}{N - n_{\mathrm{par}}} \right]^{1/2} \tag{8}$$

$$\max \left| \Delta H^{E}_{m} \right| = max \left| H^{E}_{\mathrm{m,exp}} - H^{E}_{\mathrm{m,calc}} \right| \tag{9}$$

$H^{E}_{m,exp}$, $H^{E}_{m,calc}$, N and n_{par} are respectively the experimental and calculated data of H^{E}_{m}, the number of experimental points and the number of adjustable parameters used in each model (Table 3).

5 Results and Discussion

H^{E}_{m} Results for the binary mixture made up of: ethanol + 1-buOH, l2-PhE + ethanol, 2-PhE + 1-BuOH and 22EEE + 1-BuOH and the ternary systems that specifically include x_1 22MEE + x_2 1-BuOH + (1-x_1-x_2) ethanol, x_1 2ME + x_2 1-BuOH + (1-x_1 -x_2) ethanol, and x_1 2-PhE + x_2 1-BuOH + (1-x_1-x_2) ethanol were obtained at both temperatures under study (298.15 and 313.15) K. In addition, H^{E}_{m} data of the binary mixtures containing, respectively, 22MEE + ethanol; 22EEE + ethanol; 2ME + ethanol; 22MEE + 1-BuOH; 2ME + 1-BuOH; at (298.15 and 313.15) K have been documented in prior works [35–37]. The corresponding experimental results are summarized in Tables 4, 5, and 6, and their graphical representations are provided in Figs. 2, 3, 4, 5, and 6 (Table 3).

The parameters employed for the calculation of H^{E}_{m} with the modified R-K equation, NRTL, and UNIQUAC models are presented in Tables 3, 7, and 8. All thermodynamic model calculations were conducted using Microsoft Excel (Solver add-in). This software environment was employed for model fitting and optimization of parameters in the R–K, NRTL, and UNIQUAC models. Additionally, the surface areas Q_K and the relative van der Waals volumes R_K also the group interaction parameters used in this study are given in Tables 9, 10 and 11. Finally, Table 10 displays the molecular structures of the chemical substances used in this work, detailing their constituent subgroups. Predictions with the Modified UNIFAC (Dortmund) model were carried out using the publicly available parameter set [34].

5.1 Binary Mixtures

5.1.1 *ethanol + 1-BuOH*

Excess molar enthalpy for the binary mixture ethanol (1) + 1-BuOH (2) indicate an endothermic behavior ($H^{E}_{m} > 0$). A skewed curve is observed in the H^{E}_{m} plot, with maximum values of 51.5 J.mol^{-1} at $T = 298.15$ K and 44.9 J.mol^{-1} at $T = 313.15$ K, both at $x_1 = 0.55$. Among the correlative models applied, the R–K equation gives the closest agreement with experimental observations, although it remains an empirical

Table 3 Sets of parameters needed for the graphical representation of excess molar enthalpy, H_m^E/, by Redlich-Kister equation, NRTL and UNIQUAC models, for studied binary mixture ethanol (1) +1-BuOH (2), 2-PhE (1) + ethanol (2), 2-PhE (1) + 1-BuOH (2), and 22EEE (1) + 1-BuOH (2) at (298.15 and 313.15) K and at $p = 0.1$ MPa.[a]

Binary System at 298.15 K				
		Redlich-Kister	NRTL	UNIQUAC
ethanol (1) +1-BuOH (2)				
A_0	J·mol^{-1}	0.0062	0.3806	794.3
A_1		201.8	−0.2387	−522.5
A_2		55.6		
A_3		7.3		
a_{12}			0.30	
MAD (%)		0.98	0.97	3.10
$rms\Delta H_m^E$ J·mol^{-1}		0.2	0.19	0.98
MaxΔH_m^E/J·mol^{-1}		0.4	0.41	1.43
2-PhE + ethanol				
A_0	J·mol^{-1}	0.2077	567.0000	26815.0
A_1		1354.1	0.7259	323.9
A_2		−88.1		
A_3		365.4		
a_{12}			0.30	
MAD (%)		0.34	5.67	4.94
$rms\Delta H_m^E$J·mol^{-1}		0.90	12.92	11.80
MaxΔH_m^E/J·mol^{-1}		1.07	25.62	24.05
2-PhE + 1-BuOH				
A_0	J·mol^{-1}	0.2766	0.3496	140.2
A_1		2525.1	1.1258	483.3
A_2		213.3		
A_3		854.9		
a_{12}			0.30	
MAD (%)		0.74	6.66	6.96
$rms\Delta H_m^E$ J·mol^{-1}		4.5	28.57	29.71
MaxΔH_m^E/J·mol^{-1}		9.5	41.30	44.88
22EEE + 1-BuOH				
A_0	J·mol^{-1}	0.4125	0.6746	429.7
A_1		3304.4	1.3512	283.1
A_2		747.2		
A_3		126.6		
a_{12}			0.31	
MAD (%)		0.14	0.39	1.78
$rms\Delta H_m^E$J·mol^{-1}		0.8	2.5	8.9
MaxΔH_m^E/J·mol^{-1}		1.2	5.7	14.7

Table 3 (continued)

Binary Systemat 313.15 K				
		Redlich-Kister	NRTL	UNIQUAC
ethanol (1) +1-BuOH (2)				
A_0	J·mol^{-1}	0.0062	0.3963	771.7
A_1		176.1	−0.2612	−549.2
A_2		56.7		
A_3		6.1		
a_{12}			0.30	
MAD (%)		1.27	1.27	3.19
$rms\Delta H_m^E$ J·mol^{-1}		0.3	0.16	0.96
MaxΔH_m^E/J·mol^{-1}		0.3	0.36	1.38
2-PhE + ethanol				
A_0	J·mol^{-1}	0.1338	0.0846	54.3
A_1		1805.0	0.8253	369.3
A_2		−172.3		
A_3		266.3		
a_{12}			0.30	
MAD (%)		0.2	3.0	2,7
$rms\Delta H_m^E$ J·mol^{-1}		0.70	7.30	6.74
MaxΔH_m^E/J·mol^{-1}		1.14	11.74	10.61
2-PhE + 1-BuOH				
A_0	J·mol^{-1}	0.0404	0.6010	387.5
A_1		3229.2	1.1831	377.1
A_2		−400.0		
A_3		676.4		
a_{12}			0.30	
MAD (%)		0.22	2.89	3.84
$rms\Delta H_m^E$J·mol^{-1}		1.2	14.95	19.53
MaxΔH_m^E/J·mol^{-1}		1.7	22.62	29.64
22EEE + 1-BuOH				
A_0	J·mol^{-1}	0.0726	0.2909	1213.2
A_1		2661.8	1.1393	−134.6
A_2		−495.8		
A_3		159.7		
a_{12}			0.30	
MAD (%)		0.18	0.18	0.42
$rms\Delta H_m^E$J·mol^{-1}		0.8	0.84	1.84
MaxΔH_m^E/J·mol^{-1}		1.4	1.85	3.86

[a]Equivalence between parameters: NRTL A_1=t_{12} and A_2=t_{21}; UNIQUAC A_1=Du_{12}; A_2=Du_{21}

fit without molecular interpretation with an AAD values of 0.75% (298.15 K) and 1.27% (313.15 K). The NRTL model reproduces the experimental trend well, owing to its consideration of local non-random interactions that captures the different molecular environments of ethanol and 1-BuOH. UNIQUAC also provides a reasonable description by considering both size/shape and energetic interactions, but it slightly underestimates the enthalpic deviation at high ethanol fractions due to its simplified treatment of hydrogen bonding. The predictive UNIFAC method shows only qualitative agreement because it neglects specific hydroxyl–hydroxyl interactions. Therefore, its performance cannot be directly compared with that of the correlative models.

Comparison with literature data for ethanol + 1-BuOH at 298.15 K and 0.1 MPa shows good agreement with previously reported results [38]. The fitting of our model to the experimental data gave an average absolute deviation (AAD) of 5.21%, confirming its reliability in describing this binary system. At 313.15 K, no experimental data were found in the literature for this mixture, which prevents direct comparison. Nevertheless, the predictions at this temperature provide a useful reference for future studies and represent an original contribution to the thermodynamic characterization of alcohol mixtures.

5.1.2 *2-PhE + ethanol*

The H_m^E behavior of the binary mixture 2-PhE + ethanol (as outlined in Fig. 2b) reveals clear differences that can be attributed to molecular size, polarity, and hydrogen bonding capabilities. The mixture reaches a maximum of 346.2 J·mol^{-1} at $x_1 = 0.3997$ and 458.5 J·mol^{-1} at $x_1 = 0.4497$ at 298.15 and 313.15 K, respectively. These results can be explained by the balance between ethanol's lower polarity and larger molecular size compared with methanol, which favors the formation of more effective hetero-interactions with 2-PhE, leading to greater enthalpic deviations. On a molecular level, 2-PhE possesses both an ether oxygen and an aromatic phenyl group, enabling dual interaction pathways: hydrogen bonding between the hydroxyl group of ethanol and the ether oxygen, and π–π or dipolar interactions involving the phenyl ring. The cooperative contribution of these interactions stabilizes mixed molecular arrangements, enhancing positive deviations in enthalpy [39]. In particular, the disruption of self-associated hydrogen-bonding networks of ethanol, compensated by the establishment of stronger 2-PhE + ethanol specific interactions, underlies the observed maxima in H_m^E.

Among the thermodynamic models applied, the R-K equation consistently provides the best fit for the ethanol system, with RMS ΔH_m^E of 5.55 J·mol^{-1} at 298.15 K. The UNIQUAC and NRTL models also show fair agreement but with slightly higher deviations, 11.80 J·mol^{-1} and 12.92 J·mol^{-1}, respectively. In contrast, the modified UNIFAC (Dortmund) model tends to overestimate the excess molar enthalpy, reflecting its limited ability to explicitly capture directional and specific hydrogen-bonding interactions.

5.1.3 *2-PhE + 1-BuOH*

The mixture 2-PhE (1) + 1-BuOH (2) indicates an endothermic behavior ($H_m^E > 0$). The maximum excess molar enthalpy for this binary mixture is 641.0 J.mol^{-1} at $T = 298.15$ K and 812.7 J.mol^{-1} at $T = 313.15$ K, both at $x_1 = 0.45$. As an empirical model, R–K equation showed the best agreement with experimental data, although it does not account for the molecular interactions. The AAD values registered for this blend were 0.74% at 298.15 K and 0.22% at 313.15 K. At 298.15 K, The NRTL, UNIQUAC, and UNIFAC methods showed similar behavior, reproducing the experimental trend reasonably well despite their approaches. However, at 313.15 K, UNIQUAC model deviated slightly from the others, underestimating the enthalpy values when x_1 less than 0.8. At lower temperatures, the hydrogen-bonding network remains more organized, which explains why all models predict the experimental data more accurately. Increasing the temperature reduces the stability of hydrogen bonds, which justifies both the higher excess enthalpy values observed and the discrepancies between models. These differences arise from the way each model accounts for local interactions and temperature effects.

5.1.4 *22EEE + 1-BuOH*

For the binary mixture 22EEE (1) + 1-BuOH (2), positive excess molar enthalpies were observed, indicating endothermic behavior. The maximum enthalpies were 834.35 J.mol^{-1} at $T = 298.15$ K, and 677.5 J.mol^{-1} at $T = 313.15$ K. For both temperatures, the maximum enthalpies were registered at $x_1 = 0.45$. From the graphical comparison, it is remarkable that UNIFAC provided the least prediction ability compared to the R-K equation, NRTL, UNIQUAC (Fig. 2d). R-K equation predicts well at $T = 298.15$ K with ADD = 0.14%, followed by NRTL with ADD = 0.39% and UNIQUAC with ADD = 1.78%. At $T = 313.15$ K, R-D equation and NRTL again exhibited the best predictive performance (AAD = 0.18%), followed by UNIQUAC (AAD = 0.42%). The decrease of the maximum enthalpy with increasing temperature for this mixture can be explained by the molecular structure of 22EEE. This compound contains several ether groups (–O–) in addition to a hydroxyl group (–OH), which confer significant conformational flexibility and allow both intra- and intermolecular hydrogen bonding. Due to this flexible and highly polar nature, hydrogen bonds are more easily disrupted as the temperature rises. Consequently, the difference between homogeneous and heterogeneous interactions becomes less pronounced, leading to a reduction in the excess molar enthalpy values at higher temperatures.

5.2 Ternary Mixtures

The ternary systems [22MEE (1) + 1-BuOH (2) + ethanol (3)], [22EEE (1) + 1-BuOH (2) + ethanol (3)], [2ME (1) + 1-BuOH (2) + ethanol (3)], and [2-PhE (1) + 1-BuOH (2) + ethanol (3)], were obtained by introducing glycol ethers into the binary systems 1-BuOH + ethanol, and their excess molar enthalpies were

determined at 298.15 K and 313.15 K. For each ternary system, four different initial binary compositions were selected, with x_2/x_3 ratios fixed at 0.2500, 0.6667, 1.5000, and 4.0000, respectively.

The experimental results of H_m^E at 298.15 and 313.15 are reported in Table 5 and Table 6, respectively. These values were determined using Eq. (10):

$$H_{123}^E = H_{1+23}^E + (1 - x_2)H_{23}^E, \tag{10}$$

where H_{1+23}^E represents the experimental values of the ternary blends, and H_{23}^E corresponds to the R-K equation of the binary ethanol + 1-BuOH blend. The temperature and composition dependence of the ternary blends is shown in Figs. 3, 4, 5, and 6.

The experimental data were further fitted using Eq. (11):

$$H_{123}^E = H_{12}^E + H_{13}^E + H_{23}^E + x_1x_2x_3\Delta H_{123}^E \tag{11}$$

With

$$\Delta H_{123}^E = B_0 + B_1x_1 + B_2x_2 + B_3x_1^2 + B_4x_2^2 + B_5x_1x_2 + B_6x_1^3 + B_7x_2^3 \tag{12}$$

The B_i parameters were determined using the unweighted least-squares method. Additionally, ΔH_{123}^E can be also calculated with:

$$\Delta H_{123}^E = B_1x_1 + B_2x_2 + B_3x_3 \tag{13}$$

Tables 7 and 8 provide a overview of the reduction and prediction results outcomes for the ternary mixtures, based on the parameters derived from the corresponding binary systems.

5.2.1 *For 22MEE + 1-BuOH + ethanol*

Endothermic behavior was observed, as indicated by the positive excess molar enthalpy H_m^E values across the entire range of composition at the studied temperatures (Fig. 3). The maximum experimental H_m^E for this blend is 889.9 J·mol^{-1} at 298.15 K and 941.7 J·mol^{-1} at 315.15 K corresponding to $x_1 = 0.4604$, $x_2 = 0.4277$ and $\times 3 = 0.1119$. The lowest AAD (4.9%) at T = 298.15 K was achieved with the NRTL model, comparably to ΔH_{123}^E, Eq. (12), UNIQUAC, ΔH_{123}^E, Eq. (13), and modified UNIFAC model (6.9%, 8.5%, 13.1% and 41.6%). At $T = 313.15$ K, the best AAD and RMS (7.2%, 57.8 J·mol-1) are achieved with ΔH_{123}^E, Eq. (12). Generally, ΔH_{123}^E, Eq. (13) and NRTL demonstrated comparable accuracy, both outperforming the UNIQUAC and UNIFAC models.

22MEE contains both one hydroxyl group and two ether oxygens. This dual functionality creates multiple possibilities for self-association through O–H···O hydrogen bonds. When mixed with ethanol and 1-BuOH, the strong alcohol–alcohol network is partly disrupted, while the new cross-associations do not fully compensate, leading to positive excess molar enthalpies. The longer butyl chain contributes to hydrophobic segregation, enhancing the enthalpic penalty of mixing. The

Table 4 Excess molar enthalpy, H_m^E, measured data of studied binary mixture x_1 ethanol + (1- x_1) 1-butanol, x_1 2-PhE + (1- x_1) ethanol, x_1 2-PhE + (1- x_1) 1-BuOH, and x_1 22EEE + (1- x_1) 1-BuOH at 298.15 and 313.15 K and at 0.1 MPa[a]

x_1	H_m^E/J·mol^{-1}	x_1	H_m^E/J·mol^{-1}	x_1	H_m^E/J·mol^{-1}	x_1	H_m^E/J·mol^{-1}
x_1 ethanol + (1- x_1) 1-BuOH [b]							
At 298.15 K							
0.0505	7	0.2994	38.3	0.5504	51.1	0.7999	38
0.0993	14.1	0.3500	42.5	0.5995	50.9	0.8496	31.2
0.1503	21.6	0.4002	46.0	0.6504	49.6	0.8997	22.7
0.1994	27.5	0.4499	48.6	0.7002	47.1	0.9503	12.3
0.2505	33.2	0.5005	50.06	0.7501	43.2		
At 313.15 K							
0.0506	5.5	0.2996	32.6	0.5505	44.9	0.8000	34.0
0.0993	11.8	0.3501	36.5	0.5995	44.8	0.8496	27.9
0.1504	17.9	0.4003	39.7	0.6504	43.7	0.8998	20.2
0.1995	23.3	0.4500	42.1	0.7003	41.8	0.9503	10.8
0.2505	28.4	0.5006	43.9	0.7502	38.6		
x_1 2-PhE + (1- x_1) ethanol [b]							
At 298.15 K							
0.0502	99.0	0.2993	331.4	0.5497	327.2	0.8007	203.1
0.0997	178.2	0.3494	342.4	0.5989	311.9	0.8510	163.0
0.1494	237.7	0.3997	346.2	0.6496	292.2	0.8989	117.5
0.1993	281.7	0.4495	344.4	0.6998	267.9	0.9495	62.8
0.2498	312.6	0.5003	338.4	0.7487	239.1		
At 313.15 K							
0.0502	118.6	0.2994	424.3	0.5498	438.2	0.8008	266.1
0.0998	212.4	0.3495	445.8	0.5989	416.0	0.8510	210.6
0.1495	288.8	0.3997	455.9	0.6498	387.9	0.8989	150.6
0.1994	347.8	0.4497	458.5	0.6998	355.5	0.9495	80.5
0.2499	393.0	0.5003	451.7	0.7488	313.7		
x_1 2-PhE + (1- x_1) 1-BuOH [b]							
At 298.15 K							
0.0502	190.9	0.3000	605.6	0.5493	625.2	0.7991	409.7
0.1000	335.1	0.3497	626.2	0.5999	583.4	0.8504	333.1
0.1504	445.3	0.3998	638.2	0.6503	554.2	0.8996	241.8
0.2002	520.5	0.4500	641.0	0.6991	518.4	0.9501	125.2
0.2492	571.1	0.5005	637.6	0.7491	469.4		
At 313.15 K							
0.0502	202.9	0.3000	746.3	0.5494	788.2	0.7991	507.9
0.1000	369.4	0.3498	784.8	0.5999	756.6	0.8504	404.3
0.1504	505.7	0.3998	807.4	0.6504	711.7	0.8996	293.2
0.2002	610.6	0.4501	812.7	0.6991	659.4	0.9501	154.9
0.2493	689.0	0.5004	806.6	0.7492	588.7		

Table 4 (continued)

x_1	H_m^E/J·mol^{-1}	x_1	H_m^E/J·mol^{-1}	x_1	H_m^E/J·mol^{-1}	x_1	H_m^E/J·mol^{-1}
x_1*22EEE* + (*1- x*$_1$) *1-BuOH* [b]							
At 298.15 K							
0.04960	203.12	0.30048	761.23	0.55038	803.45	0.79983	487.62
0.09945	373.76	0.34958	801.92	0.60003	767.77	0.84904	386.69
0.14951	508.92	0.40000	825.43	0.64942	717.70	0.89940	271.39
0.19975	616.87	0.45025	834.35	0.69987	652.66	0.94914	142.95
0.25006	700.26	0.50041	826.08	0.75007	576.29		
At 313.15 K							
0.0503	164.6	0.2997	623.2	0.5494	642.1	0.7997	371.2
0.0999	302.9	0.3500	657.3	0.5996	608.3	0.8506	290.3
0.1496	414.8	0.3996	673.5	0.6487	562.7	0.8994	201.8
0.1995	503.2	0.4500	676.5	0.6995	509.5	0.9499	104.3
0.2491	572.9	0.4995	666.7	0.7486	446.0		

[a]Standard uncertainties of pressure p, temperature T and mole fraction x are as follows: $u(p) = 0.01$ MPa, $u(T) = 0.05$ K, $u(x) = 0.0008$. The relative expanded uncertainty ($k = 2$) is $U_r(H^E) = 0.01$ for excess enthalpy

[b]x_1 is the mole fraction of ethanol, 2-PhE, or 22EEE

Dortmund-UNIFAC model gives poor predictions, which reflects its inability to treat the balance between multiple association sites and hydrophobic mismatch.

5.2.2 *For 22EEE + 1-BuOH + ethanol*

A similar endothermic behavior was observed for the mixture 22EEE + 1-BuOH + ethanol, supported by positive H_m^E values at the two investigated temperatures, as shown in Fig. 4. The maximum excess molar enthalpy H_m^E for this blend is 791.3 J·mol^{-1} at 298.15 K and 830.6 J·mol^{-1} at 313.15 K corresponding to $x_1 = 0.4348$, $x_2 = 0.4484$ and $x_3 = 0.1168$. At 298.15 K, the NRTL model gives the best representation of the experimental data, with the lowest deviations in terms of AAD (5.717%), RMS (40.3 J·mol^{-1}), and Max $|\Delta H_m^E|$ (110.0 J·mol^{-1}). A similar trend is observed at 313.15 K, where NRTL again provides the smallest errors (AAD = 6.2%, RMS = 56.4 J·mol^{-1}, Max $|\Delta H_m^E| = 123.7$ J·mol^{-1}). These results confirm that the NRTL model is the most reliable among those tested for describing the thermodynamic behavior of the system at both temperatures.

Structurally, 22EEE differs from 22MEE by the presence of an ethyl instead of a methyl substituent, which increases hydrophobicity and slightly reduces the polarity of the molecule. This weaker polarity results in less cohesive self-association compared to 22MEE, which explains the somewhat lower magnitude of H_m^E. However, mixing still requires breaking strong ethanol–butanol hydrogen-bonded structures, and the newly formed hetero-associations remain energetically unfavorable overall. The UNIFAC (Dortmund) model performs poorly for this system as well, showing

Table 5 Experimental data of H^E_{1+23} at 298.15 K and at 0.1 MPa for ternary mixtures: x_1 22MEE + x_2 1-BuOH + (1-x_1-x_2) ethanol, x_1 2ME + x_2 1-BuOH + (1-x_1-x_2) ethanol, and x_1 2-PhE + x_2 1-BuOH + (1-x_1-x_2) ethanol and values of H^E_{123} obtained with Eq. (11), using the smoothed representation of H^E_{23} by the modified Redlich–Kister equation with parameters given in Table 3.[a,b]

x_1	H^E_{1+23}*/J.mol^{-1}	H^E_{123}*/J.mol^{-1}	x_1	H^E_{1+23}/J.mol^{-1}	H^E_{123}/J.mol^{-1}
x*$_1$*22MEE* + ***x*$_2$*1-BuOH* + (*1*-x*$_1$-***x*$_2$)*ethanol***					
$x_2/x_3 = 0.2500$; H^E_{23}/J.mol^{-1} = 27.3					
0.1245	390.2	414.1	0.6586	586.0	595.3
0.2426	541.3	562.0	0.7495	516.5	523.4
0.3549	621.1	638.7	0.8367	427.3	431.7
0.4612	646.6	661.3	0.9212	319.8	321.9
0.5620	631.9	643.9			
$x_2/x_3 = 0.6667$; H^E_{23}/J.mol^{-1} = 45.5					
0.1161	419.7	460.0	0.6389	667.0	683.4
0.2274	587.2	622.4	0.7326	589.8	601.9
0.3352	683.1	713.4	0.8254	483.3	491.3
0.4393	720.9	746.5	0.9136	355.9	359.8
0.5403	713.5	734.4			
$x_2/x_3 = 1.5000$; H^E_{23}/J.mol^{-1} = 51.2					
0.1254	478.8	523.5	0.6603	715.7	733.0
0.2446	665.8	704.4	0.7509	625.6	638.3
0.3564	761.7	794.6	0.8377	508.0	516.4
0.4625	793.2	820.7	0.9203	367.7	371.8
0.5635	774.8	797.1			
$x_2/x_3 = 4.0000$; H^E_{23}/J.mol^{-1} = 38.8					
0.1240	520.9	554.9	0.6567	788.8	802.1
0.2424	724.4	753.8	0.7482	688.2	697.9
0.3532	831.0	856.1	0.8366	555.6	562.0
0.4604	869.0	889.9	0.9201	393.1	396.2
0.5607	851.7	868.7			
x*$_1$*22EEE* + ***x*$_2$*1-BuOH* + (*1*-x*$_1$-***x*$_2$)*ethanol***					
$x_2/x_3 = 0.2500$; H^E_{23}/J.mol^{-1} = 27.3					
0.1136	334.9	359.1	0.6341	531.6	541.6
0.2235	458.5	479.7	0.7292	486.3	493.6
0.3297	529.0	547.3	0.8213	424.9	429.8
0.4337	559.3	574.7	0.9129	348.1	350.5
0.5347	558.5	571.2			
$x_2/x_3 = 0.6667$; H^E_{23}/J.mol^{-1} = 45.5					
0.1137	380.3	420.6	0.6337	592.2	608.8
0.2236	519.4	554.7	0.7290	536.3	548.6
0.3309	597.6	628.1	0.8207	462.5	470.6
0.4347	629.1	654.8	0.9115	369.9	373.9
0.5349	625.0	646.2			
$x_2/x_3 = 1.5000$; H^E_{23}/J.mol^{-1} = 51.2					
0.1120	410.5	455.9	0.6309	644.7	663.6
0.2217	563.5	603.3	0.7256	582.2	596.2

Table 5 (continued)

x_1	$H^E_{1+23}{}^*$/J.mol^{-1}	$H^E_{123}{}^*$/J.mol^{-1}	x_1	H^E_{1+23}/J.mol^{-1}	H^E_{123}/J.mol^{-1}
0.3283	650.3	684.6	0.8200	495.2	504.4
0.4320	686.1	715.2	0.9112	388.0	392.5
0.5320	681.8	705.7			
$\frac{x_2}{x_3} = 4.0000; H^E_{23}$/J.mol^{-1} = 38.8					
0.1130	467.6	502.0	0.6340	716.3	730.5
0.2242	639.4	669.5	0.7293	640.6	651.1
0.3303	731.9	757.9	0.8214	538.8	545.7
0.4348	769.4	791.3	0.9112	412.7	416.2
0.5349	761.9	779.9			
x_1*2ME* + x_2*1-BuOH* + (*1-*x_1-x_2)*ethanol*					
$x_2/x_3 = 0.2500$; H^E_{23}/J.mol^{-1} = 27.3					
0.0996	298.8	323.3	0.5998	522.9	533.8
0.1999	412.9	434.7	0.6992	476.2	484.4
0.3004	489.0	508.1	0.8006	401.0	406.4
0.3996	530.8	547.2	0.8993	302.5	305.2
0.4999	541.6	555.2			
$x_2/x_3 = 0.6667$; H^E_{23}/J.mol^{-1} = 45.4					
0.1005	341.2	382.1	0.6005	597.8	616.0
0.1992	472.2	508.6	0.6993	541.9	555.6
0.3000	561.5	593.3	0.8001	451.0	460.1
0.4000	609.4	636.7	0.8999	329.6	334.1
0.4992	621.3	644.1			
$x_2/x_3 = 1.500$; H^E_{23}/J.mol^{-1} = 51.2					
0.1003	382.5	428.5	0.5998	674.1	694.6
0.1995	531.6	572.6	0.7003	608.0	623.4
0.3003	632.5	668.2	0.7994	504.2	514.4
0.3998	687.3	718.0	0.9003	358.5	363.6
0.4998	701.2	726.8			
$\frac{x_2}{x_3} = 4.0000; H^E_{23}$/J.mol^{-1} = 38.8					
0.0929	408.1	443.3	0.5802	761.5	777.8
0.1877	573.8	605.3	0.6826	693.3	705.6
0.2827	687.9	715.7	0.7864	575.6	583.9
0.3808	757.5	781.5	0.8926	403.7	407.8
0.4790	782.1	802.3			
x_1*2-PhE* + x_2*1-BuOH* + (*1-*x_1-x_2)*ethanol*					
$x_2/x_3 = 0.2500$; H^E_{23}/J.mol^{-1} = 27.3					
0.1492	349.9	373.0	0.7023	446.8	454.9
0.2831	454.9	474.5	0.7861	401.7	407.5
0.4037	494.0	510.3	0.8627	342.9	346.6
0.5130	496.5	509.8	0.9347	268.8	270.5
0.6119	478.4	489.0			
$x_2/x_3 = 0.6667$; H^E_{23}/J.mol^{-1} = 45.5					
0.1002	414.5	455.5	0.5989	667.0	685.2
0.2005	568.2	604.6	0.6999	621.8	635.4

Table 5 (continued)

x_1	$H^{E}_{1+23}{}^{*}$/J.mol^{-1}	$H^{E}_{123}{}^{*}$/J.mol^{-1}	x_1	H^{E}_{1+23}/J.mol^{-1}	H^{E}_{123}/J.mol^{-1}
0.3007	646.7	678.5	0.7992	547.9	557.1
0.3992	679.8	707.2	0.8997	438.0	442.5
0.5001	686.0	708.8			
$x_2/x_3 = 1.5000$;H^{E}_{23}/J.mol^{-1} = 51.2					
0.1003	456.1	502.1	0.5995	726.8	747.3
0.1998	622.4	663.3	0.6996	677.7	693.1
0.3001	706.0	741.8	0.7990	593.2	603.5
0.3994	742.6	773.3	0.9009	464.6	469.7
0.5001	748.7	774.3			
$x_2/x_3 = 4.0000$;H^{E}_{23}/J.mol^{-1} = 38.8					
0.0995	498.3	533.2	0.6000	787.2	802.7
0.1994	677.8	708.8	0.6994	732.3	743.9
0.3000	766.8	793.9	0.7991	640.9	648.7
0.4001	804.3	827.6	0.9001	494.6	498.5
0.5000	810.3	829.6			

[*] H^{E}_{1+23}: excess enthalpy (enthalpy of mixing) of component 1 with binary mixture composed of component 2 and 3;H^{E}_{123}: experimental excess enthalpy derived from experimental values of$H^{E}_{1+23}$and$H^{E}_{23}$by Eq. (10)

[a]Standard uncertainties of pressure p, temperature T and mole fraction x *and* x_2/x_3 are as follows: $u(p) = 0.01$ MPa, $u(T) = 0.05$ K, $u(x) = 0.0008$, $u(x_2/x_3) = 0.001$ (estimated by error propagation). The relative expanded uncertainty ($k = 2$) is $U_r(H^E) = 0.01$ for excess enthalpy

[b]22MEE: 2-(2-MethoxyEthoxy)Ethanol; 22EEE: 2-(2-EthoxyEthoxy)Ethanol; 2ME: 2-Methoxyethanol; 2-PhE: 2-Phenoxyethanol; 1-BuOH: 1-Butanol

that this model do not capture the subtle differences in chain length and polarity that strongly influence association equilibria.

5.2.3 *For 2ME + 1-BuOH + ethanol*

The 2ME + 1-BuOH + ethanol blend also showed endothermic behavior with positive H^E_m values over the entire composition rangeat both temperatures considered (Fig. 5). The maximum excess molar enthalpy H^E_m is 802.3 J·mol^{-1} at 298.15 K and 844.9 J·mol^{-1}, at 313.15 K related to $x_1 = 0.4791$, $x_2 = 0.4133$ and $x_3 = 0.1077$. The minimum AAD (5.7%), RMS (37.9 J·mol^{-1}) and Max $|\Delta H^E_m|$ (89.5 J·mol^{-1}) at T = 298.15 K, are registered for NRTL, compared to ΔH^E_{123}, Eq. (12), ΔH^E_{123}, Eq. (13) and UNIQUAC. At T = 313.15 K, ΔH^E_{123}, Eq. (12) and NRTL model are the best with AAD (6.4%, 6.5%), RMS (45.0 J·mol^{-1}, 45.0 J·mol^{-1}) and Max $|\Delta H^E_m|$ (118.1 J·mol^{-1}, 114.0 J·mol^{-1}). These models demonstrated better accuracy than UNIQUAC and UNIFAC models.

2ME is smaller than the diethylene glycol monoethers (22MEE, 22EEE) and has only one ether oxygen, yet it still forms strong hydrogen-bonded structures. On mixing, disruption of ethanol–ethanol and ethanol–butanol associations leads to a positive enthalpy, but the magnitude is lower than for 22MEE because the steric hindrance is less pronounced and cross-interactions with ethanol are more favorable.

Table 6 Experimental data of H^E_{1+23} at 313.15 K and at 0.1 MPa for ternary mixtures: $x_1$22MEE + $x_2$1-BuOH + (1-x_1-x_2) ethanol, $x_1$2ME + $x_2$1-BuOH + (1-x_1-x_2) ethanol, and $x_1$2-PhE + $x_2$1-BuOH + (1-x_1-x_2) ethanol and values of H^E_{123}obtained with Eq. (11), using the smoothed representation of $H^E_{23}$by the modified Redlich–Kister equation with parameters given in Table 3.[a,b]

x_1	$H^E_{1+23}{}^*$/J.mol^{-1}	$H^E_{123}{}^*$/J.mol^{-1}	x_1	H^E_{1+23}/J.mol^{-1}	H^E_{123}/J.mol^{-1}
$x_1$22MEE + $x_2$1-BuOH + (1-x_1-x_2) ethanol					
$x_2/x_3 = 0.2500$;H^E_{23}/J.mol^{-1} = 23.0					
0.1245	414.1	434.2	0.6586	624.5	632.3
0.2427	576.6	594.0	0.7495	548.9	554.7
0.3549	661.8	676.6	0.8367	453.8	457.5
0.4612	689.8	702.2	0.9212	340.6	342.5
0.5620	674.0	684.1			
$x_2/x_3 = 0.6667$;H^E_{23}/J.mol^{-1} = 39.3					
0.1161	437.6	472.3	0.6389	700.8	715.0
0.2275	614.1	644.4	0.7342	618.7	629.1
0.3365	716.3	742.3	0.8254	508.0	514.9
0.4408	758.8	780.7	0.9136	375.6	379.0
0.5418	749.2	767.2			
$x_2/x_3 = 1.5000$;H^E_{23}/J.mol^{-1} = 45.0					
0.1241	501.0	540.4	0.6573	759.2	774.6
0.2433	701.8	735.9	0.7494	661.6	672.9
0.3549	807.5	836.5	0.8361	536.3	543.7
0.4610	842.6	866.9	0.9203	387.4	391.0
0.5620	823.2	842.9			
$x_2/x_3 = 4.0000$;H^E_{23}/J.mol^{-1} = 34.6					
0.1241	548.9	579.3	0.6582	830.8	842.6
0.2423	764.4	790.6	0.7498	720.8	729.4
0.3547	882.4	904.7	0.8366	581.3	587.0
0.4604	923.0	941.7	0.9201	412.3	415.0
0.5622	900.8	915.9			
$x_1$22EEE + $x_2$1-BuOH + (1-x_1-x_2)ethanol					
$x_2/x_3 = 0.2500$;H^E_{23}/J.mol^{-1} = 23.0					
0.1136	351.1	371.4	0.6341	569.6	578.0
0.2235	483.2	501.1	0.7292	521.4	527.6
0.3311	561.6	577.0	0.8213	455.7	459.8
0.4352	596.3	609.3	0.9129	373.9	375.9
0.5364	596.3	607.0			
$x_2/x_3 = 0.6667$;H^E_{23}/J.mol^{-1} = 37.2					
0.1157	401.4	434.2	0.6371	628.2	641.7
0.2270	551.7	580.4	0.7328	568.4	578.3
0.3347	635.0	659.7	0.8248	488.7	495.2
0.4390	670.2	691.0	0.9137	393.2	396.4
0.5396	664.5	681.6			

Table 6 (Continued)

x_1	$H^{E}_{1+23}{}^{*}$/J.mol^{-1}	$H^{E}_{123}{}^{*}$/J.mol^{-1}	x_1	H^{E}_{1+23}/J.mol^{-1}	H^{E}_{123}/J.mol^{-1}
$x_2/x_3 = 1.5000; H^{E}_{23}$/J.mol$^{-1} = 45.0$					
0.1120	441.1	481.0	0.6308	682.7	699.3
0.2216	608.6	643.6	0.7273	613.7	626.0
0.3283	703.1	733.4	0.8200	522.5	530.6
0.4321	742.7	768.3	0.9112	411.1	415.1
0.5320	735.6	756.7			
$x_2/x_3 = 4.0000; H^{E}_{23}$/J.mol$^{-1} = 34.6$					
0.1141	483.8	514.5	0.6340	753.0	765.7
0.2241	664.7	691.6	0.7292	671.8	681.1
0.3315	768.6	791.8	0.8214	565.8	571.9
0.4348	811.1	830.6	0.9131	432.9	435.9
0.5364	800.9	816.9			
x_1*2ME +* x_2*1-BuOH +* (=1-x_1-x_2)*ethanol*					
$x_2/x_3 = 0.2500; H^{E}_{23}$/J.mol$^{-1} = 23.3$					
0.0996	321.3	342.0	0.5999	557.5	566.7
0.1998	443.3	461.7	0.6991	506.7	513.6
0.2990	524.2	540.3	0.7990	428.5	433.1
0.3996	568.7	582.5	0.8994	323.1	325.4
0.4999	578.5	590.0			
$x_2/x_3 = 0.6667; H^{E}_{23}$/J.mol$^{-1} = 39.3$					
0.1019	366.2	401.5	0.6034	628.9	644.5
0.2020	503.6	535.0	0.7037	566.4	578.0
0.3028	597.6	625.0	0.8032	471.4	479.2
0.4043	647.0	670.4	0.9014	345.9	349.8
0.5036	656.7	676.2			
$x_2/x_3 = 1.5000; H^{E}_{23}$/J.mol$^{-1} = 45.0$					
0.1003	407.3	447.7	0.5999	710.7	728.7
0.1994	565.1	601.1	0.7003	638.9	652.3
0.3002	671.9	703.4	0.7994	528.5	537.5
0.3999	729.3	756.3	0.9003	377.0	381.5
0.4998	741.5	764.0			
$x_2/x_3 = 4.0000; H^{E}_{23}$/J.mol$^{-1} = 34.6$					
0.0929	433.9	465.3	0.5801	801.6	816.1
0.1876	609.0	637.1	0.6825	726.2	737.2
0.2827	731.5	756.2	0.7863	601.5	608.8
0.3808	803.7	825.1	0.8926	422.9	426.6
0.4791	826.9	844.9			

Table 6 (Continued)

x_1	H^{E}_{1+23} */J.mol^{-1}	H^{E}_{123} */J.mol^{-1}	x_1	H^{E}_{1+23}/J.mol^{-1}	H^{E}_{123}/J.mol^{-1}
x_1*2-PhE +* x_2*1-BuOH + (1-*x_1*-*x_2 *)ethanol*					
$x_2/x_3 = 0.2500$;H^{E}_{23}/J.mol^{-1} = 23.0					
0.0998	601.4	622.1	0.5985	1006.4	1015.7
0.1998	792.4	810.8	0.6990	968.2	975.2
0.2997	913.7	929.8	0.7988	897.8	902.4
0.3996	983.1	996.9	0.9005	793.6	795.9
0.4991	1012.7	1024.2			
$x_2/x_3 = 0.6667$;H^{E}_{23}/J.mol^{-1} = 39.3					
0.1005	669.4	704.7	0.6012	1090.8	1106.4
0.2006	877.9	909.3	0.7003	1040.1	1051.8
0.3009	1008.6	1036.0	0.7996	955.1	963.0
0.4011	1079.8	1103.3	0.8999	826.5	830.4
0.5005	1106.6	1126.2			
$x_2/x_3 = 1.5000$;H^{E}_{23}/J.mol^{-1} = 45.0					
0.1002	506.6	547.1	0.5996	876.3	894.3
0.1999	717.9	753.9	0.6996	802.4	815.9
0.2989	842.8	874.3	0.7991	686.5	695.5
0.3994	902.6	929.6	0.8987	521.5	526.0
0.4986	911.7	934.3			
$x_2/x_3 = 4.0000$;H^{E}_{23}/J.mol^{-1} = 34.6					
0.0995	551.3	582.5	0.5985	953.2	967.1
0.1995	783.5	811.2	0.6995	869.6	880.0
0.2989	919.1	943.4	0.7991	740.1	747.1
0.3989	982.6	1003.4	0.9002	550.6	554.1
0.4986	991.1	1008.5			

*H^{E}_{1+23}: excess enthalpy (enthalpy of mixing) of component 1 with binary mixture composed of component 2 and 3; H^{E}_{123}: experimental excess enthalpy derived from experimental values of H^{E}_{1+23} and $H^{E}_{23}$by equation (10).

[a]Standard uncertainties of pressure p, temperature T and mole fraction x *and* x_2/x_3 are as follows: $u(p)$= 0.01 MPa, $u(T) = 0.05$ K, $u(x) = 0.0008$, $u(x_2/x_3) = 0.001$ (estimated by error propagation). The relative expanded uncertainty ($k = 2$) is $U_r(H^E) = 0.01$ for excess enthalpy.

[b]22MEE: 2-(2-MethoxyEthoxy)Ethanol; 22EEE: 2-(2-EthoxyEthoxy)Ethanol 2ME: 2-Methoxyethanol; 2-PhE: 2-Phenoxyethanol; 1-BuOH: 1-Butanol

The modified UNIFAC approach again shows significant errors, which highlights its limitation in representing size-dependent and polarity-driven interactions.

5.2.4 *For 2-PhE + 1-BuOH + ethanol*

For the 2-PhE + 1-BuOH + ethanol blend, endothermic behavior was confirmed by positive H^{E}_{m} values for all mole fractions at both investigated temperatures (Fig. 6). The maximum excess molar enthalpy H^{E}_{m} was 829.6 J·mol^{-1} at 298.15 K and increased to 1126.2 J·mol^{-1} at 315.15 K corresponding to $x_1 = 0.5005$, $x_2 = 0.1961$ and $x_3 = 0.3033$. At 298.15 K, ΔH^{E}_{123}, Eq. (12) has the lowest ADD and RMS (8.1%,

60.9 J·mol^{-1}), while the lowest Max |Δ H_m^E| is registered for NRTL (165.3 J·mol^{-1}). At T = 313.15 K, the minimum AAD (6.2%), RMS (56.4 J·mol^{-1}) and Max |Δ H_m^E| (123.7 J·mol^{-1}), are found for NRTL model.

The strong endothermicity of this system originates from the molecular features of 2-PhE. The aromatic ring introduces π–π interactions and increases the hydrophobicity of the molecule, making it less compatible with ethanol and 1-BuOH. When the mixture forms, both the aromatic self-association of 2-PhE and the hydrogen-bonded alcohol structures are disrupted, but the cross-interactions are not strong enough to compensate. This results in the highest positive H_m^E values among the systems studied. The UNIFAC (Dortmund) model fails drastically (AAD above 74.6%), mainly because the group parameters do not explicitly account for aromatic-specific interactions or the anisotropy of phenoxy substitution.

For the ternary blends of 22MEE + 1-BuOH + ethanol and 22EEE + 1-BuOH + ethanol at 298.15 K, the NRTL model provides the best agreement with experimental data compared to UNIQUAC and UNIFAC. At 313.15 K, NRTL again gives the lowest deviations for the system containing 22MEE, with AAD = 22.5%, RMS = 67.6 J·mol^{-1}, and Max |Δ H_m^E |= 131.6 J·mol^{-1}. For the mixture with 22EEE at the same temperature, the deviations obtained with NRTL are AAD = 19.57%, RMS = 62.1 J·mol^{-1}, and Max |Δ H_m^E|= 148.1 J·mol^{-1}. However, for this blend at 313.15 K, UNIQUAC outperforms the other models, yielding the lowest deviations (AAD = 29.12%, RMS = 206.2 J·mol^{-1}, Max |Δ H_m^E|= 476.7 J·mol^{-1}). UNIQUAC also shows the best performance at 298.15 K for the 2ME + 1-BuOH + ethanol system (AAD = 19.3%, RMS = 74.8 J·mol^{-1}, Max |Δ H_m^E|= 159.3 J·mol^{-1}) and for the 2-PhE + 1-BuOH + ethanol system (AAD = 24.1%, RMS = 113.2 J·mol^{-1}), although in the latter case NRTL gives the lowest Max |Δ H_m^E| (275.5 J·mol^{-1}). At 313.15 K, the NRTL model performs better for the 2ME + 1-BuOH + ethanol mixture, with the lowest RMS (136.1 J·mol^{-1}) and Max |Δ H_m^E| (190.5 J·mol^{-1}), while its AAD (31.4%) is nearly identical to that of UNIQUAC. For the 2-PhE + 1-BuOH + ethanol blend at this temperature, the UNIQUAC model provides the most accurate prediction, with the smallest deviations (AAD = 29.1%, RMS = 206.2 J·mol^{-1}, Max |Δ H_m^E|= 476.3 J·mol^{-1}).

Table 10 presents the molecular formulae of the species studied, illustrated as subgroups structures used in group-contribution models. The studied liquids differ in molecular size, shape, and interaction potential. Across all ternary mixtures, positive H_m^E values confirmed endothermic behavior, attributed to weak intermolecular interactions. At constant pressure, excess molar enthalpy increased as temperature rose from 298.15 K to 323.15 K in all mixture: 22MEE + 1-BuOH + ethanol, 22EEE + 1- BuOH + ethanol, 2ME + 1- BuOH + ethanol, 2-PhE + 1- BuOH + ethanol. This increase is likely due to the relatively low polarity and weak associative interactions among the molecules. As temperature increases, hydrogen bonds (alcohol–alcohol and alcohol–ether) weaken, leading to an increase in H_m^E. Glycol ethers improve miscibility between highly polar ethanol and less polar butanol. However, at higher temperatures, the effect of glycol ethers is reduced, weakening dipolar interactions and contributing to increased excess molar enthalpy.

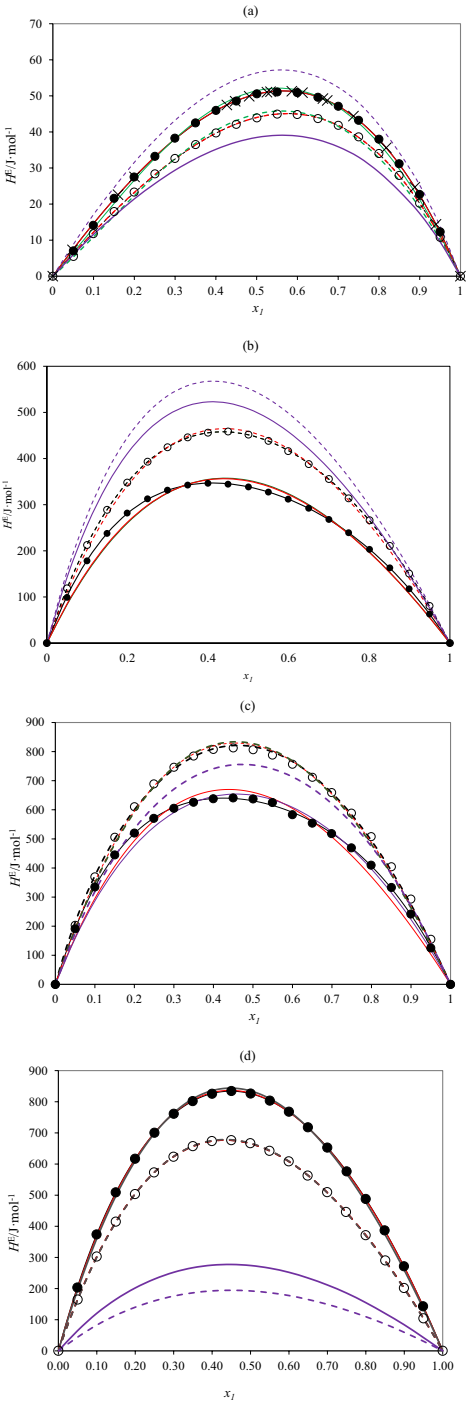

Fig. 2 Excess molar enthalpy H_m^E of (**a**) ethanol (1) + 1-BuOH (2); **b** 2-PhE (1) + ethanol (2); **c** 2-PhE (1) + 1-BuOH (2); and 22EEE (1) + 1-BuOH (2). At $T = 298.15$ K: (●), experimental data; (+) A. E. Pope et al. [38]; (——), calculated values with modified Redlich–Kister equation; (——), calculated values with NRTL model, (——), calculated values with UNIQUAC model, (——), calculated values with UNIFAC model. At $T = 313.15$ K: (○), experimental data; (—), calculated values with modified Redlich–Kister equation; (—), calculated values with NRTL model, (—), calculated values with UNIQUAC model, (—), calculated values with UNIFAC model

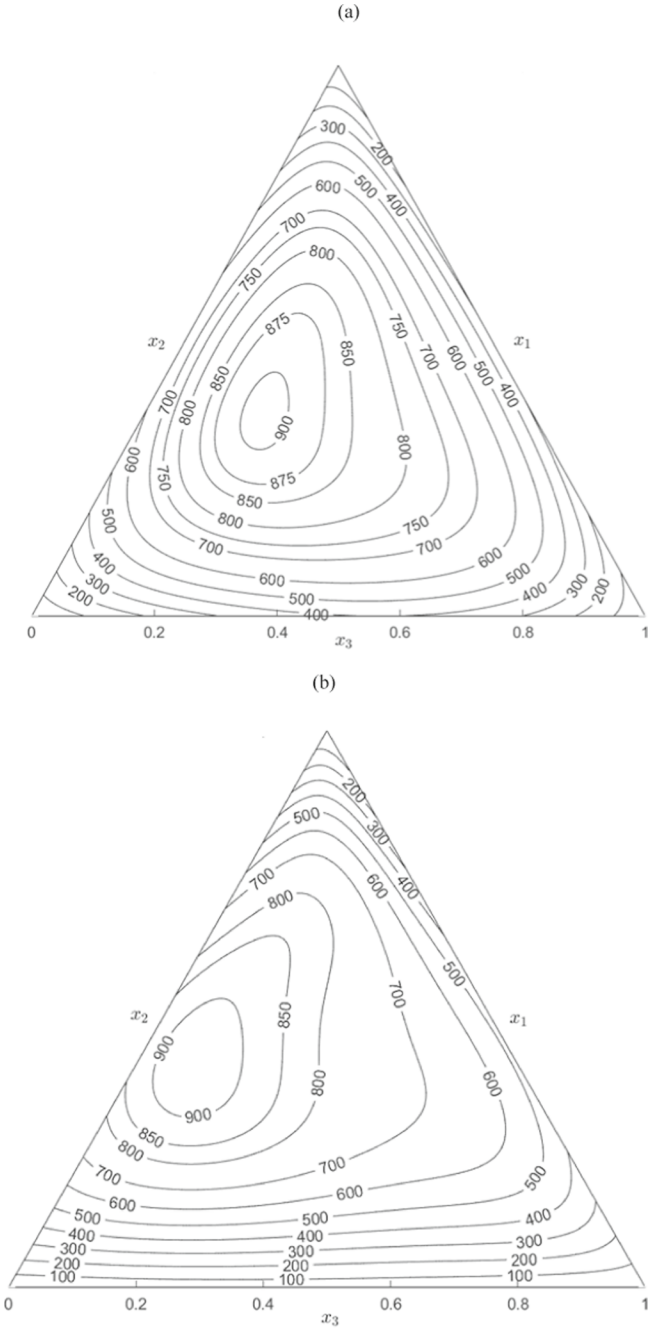

Fig. 3 Contours for constant values of H^E_{123} for ternary mixture 22MEE (1) + 1-BuOH (2) + ethanol (3), calculated from the representation of the experimental results by Eqs. (12 and 13) using the parameters given in Tables 7 and 8: (a), at 298.15 K; (b), at 313.15 K. This figure is plotted using MATLAB Simulink

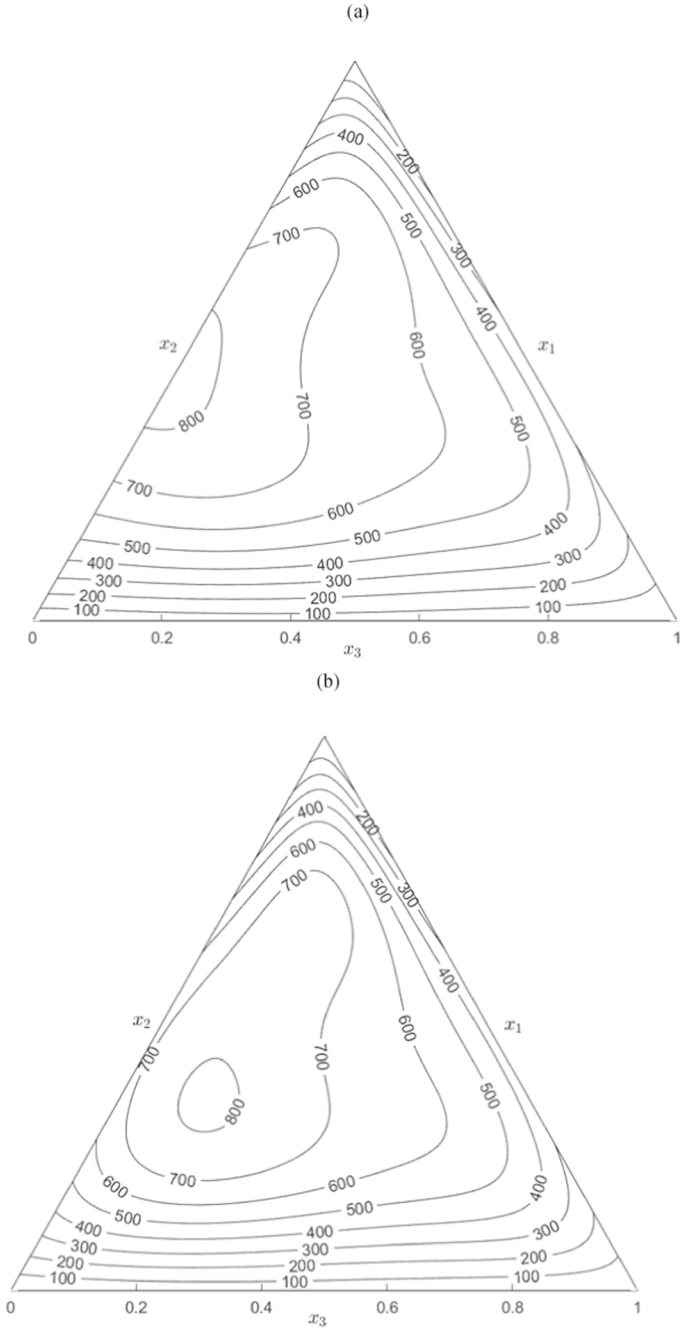

Fig. 4 Contours for constant values of H^E_{123} for ternary mixture 22EEE (1) + 1-BuOH (2) + ethanol (3), calculated from the representation of the experimental results by Eqs. (12 and 13) using the parameters given in Tables 7 and 8: (a), at 298.15 K; (b), at 313.15 K. This figure is plotted using MATLAB Simulink

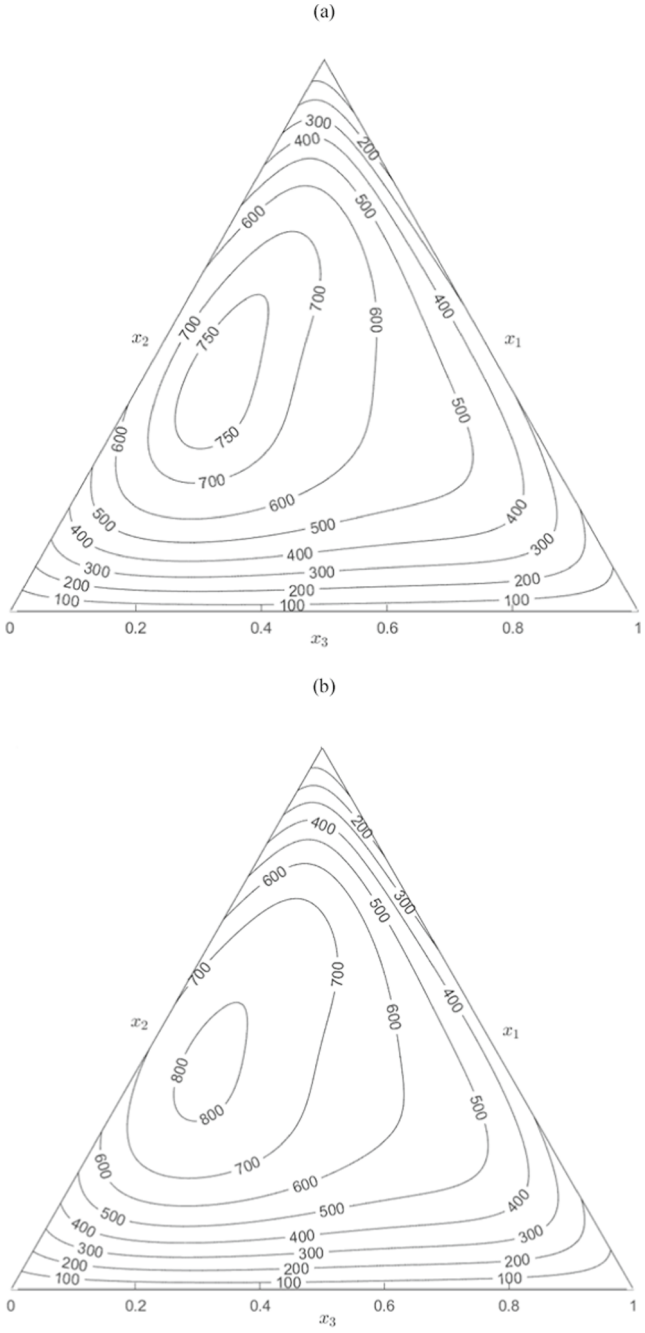

Fig. 5 Contours for constant values of H^E_{123} for ternary mixture 2ME (1) + 1-BuOH (2) + ethanol (3), calculated from the representation of the experimental results by Eqs. (12 and 13) using the parameters given in Tables 7 and 8: **a**, at 298.15 K; **b**, 313.15 K. This figure is plotted using MATLAB Simulink

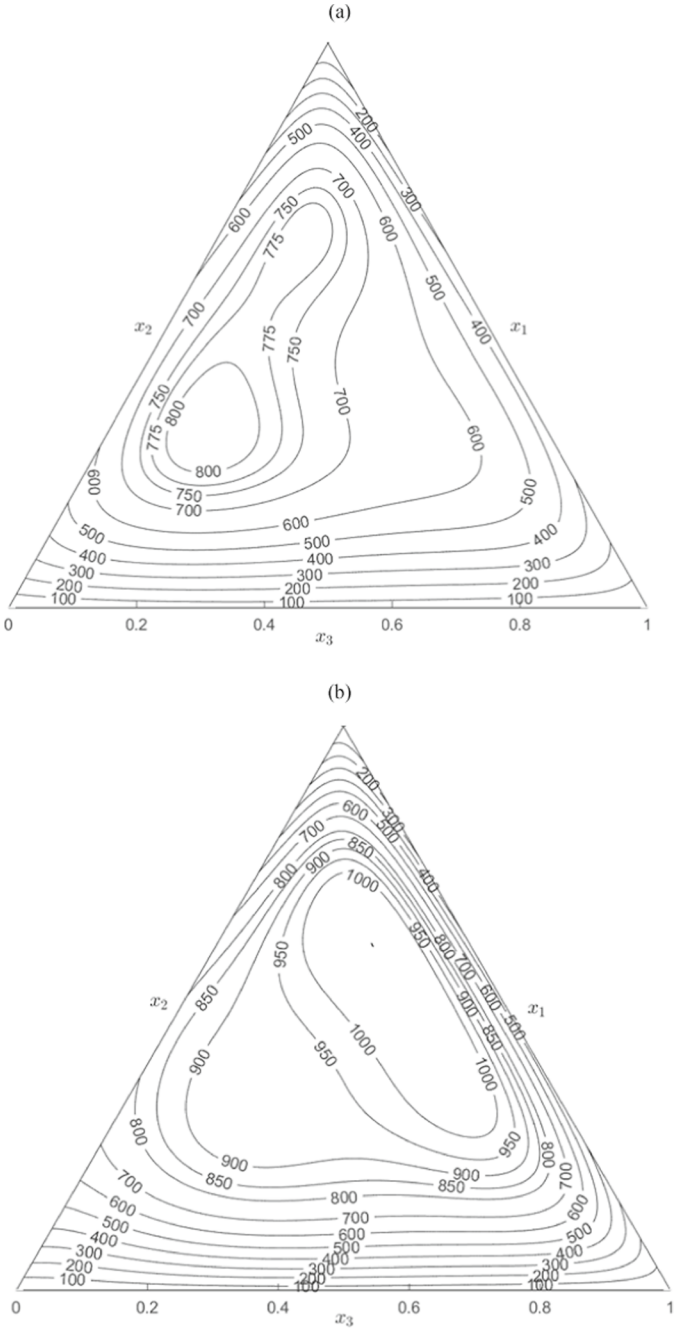

Fig. 6 Contours for constant values of H^E_{123} for ternary mixture 2PhE (1) + 1-BuOH (2) + ethanol (3), calculated from the representation of the experimental results by Eqs. (12 and 13) using the parameters given in Tables 7 and 8: **a**, at 298.15 K; **b**, 313.15 K. This figure is plotted using MATLAB Simulink

Table 7 Summary of the data reduction and prediction results obtained for the studied ternary mixtures: 22MEE (1) + 1-BuOH (2) + ethanol (3), 22EEE (1) + 1-BuOH (2) + ethanol (3), 2ME (1) + 1-BuOH (2) + ethanol (3) and 2-PhE (1) + 1-BuOH (2) + ethanol (3) at 298.15 K and at $p = 0.1$ MPa.[a,b]

Correlation		ΔH^E_{123}, Eq. (12)	ΔH^E_{123}, Eq. (13)	NRTL	UNIQUAC
22MEE (1) + 1-BuOH (2) + ethanol (3)					
B_0	J·mol^{-1}	14620.3	14569.96	1.2016	849.61
B_1		31885.5	2081.2	1.3579	91.28
B_2		−66261.30	1872.23	2.4201	1796.85
B_3		−203333.8		4.3165	−547.63
B_4		115333.23		−0.0285	−386.09
B_5		40907.26		0.1098	650.93
B_6		240450.9			
B_7		−62898.9			
a				0.30	
MAD (%)		6.9	13.	4.9	8.5
$rms\Delta H^E_m$ /J·mol^{-1}		53.2	85.6	35.8	59.5
MaxΔH^E_m ΔH^E_m /J·mol^{-1}		145.2	187.9	104.8	132.5
22EEE (1) + 1-BuOH (2) + ethanol (3)					
B_0	J·mol^{-1}	15038.9	11763.75	0.9386	715.68
B_1		47173.6	−2235.7	1.2748	117.74
B_2		−75670.69	6476.41	2.8725	1925.49
B_3		−224396.6		4.2782	−642.98
B_4		148831.17		−0.1889	−355.97
B_5		5063.91		0.3116	627.22
B_6		247194.3			
B_7		−91458.1			
a				0.30	
MAD (%)		7.92	14.39	5.71	10.12
$rms\Delta H^E_m \Delta H^E_m$ J·mol^{-1}		58.2	92.5	40.3	68.6
MaxΔH^E_m /J·mol^{-1}		175.9	227.4	110.0	155.8
2ME (1) + 1-BuOH (2) + ethanol (3)					
B_0	J·mol^{-1}	25769.3	13537.10	0.7827	578.56
B_1		−25236.5	8537.6	0.7668	416.50
B_2		−88815.59	1994.95	2.3364	930.75
B_3		−86623.0		7.6898	−119.94
B_4		127822.56		1.5008	1315.75
B_5		81660.35		−0.8119	−745.10
B_6		155813.1			
B_7		−44930.5			
a				0.20	
MAD (%)		6.45	13.21	5.7	7.57

Table 7 (continued)

Correlation		ΔH^E_{123}, Eq. (12)	ΔH^E_{123}, Eq. (13)	NRTL	UNIQUAC
$rms\Delta H^E_m \Delta H^E_m$ J·mol^{-1}		42.6	77.2	37.9	49.2
MaxΔH^E_m /J·mol^{-1}		111.5	165.1	89.5	100.7
2-PhE (1) + 1-BuOH (2) + ethanol (3)					
B_0	J·mol^{-1}	1791.3	17625.30	0.6708	751.89
B_1		42668.6	12843.0	1.3227	372.97
B_2		46367.23	−2537.55	3.0628	1652.41
B_3		−254221.1		8.0632	−547.96
B_4		−150327.07		0.3898	1336.54
B_5		40190.39		−0.1931	−698.56
B_6		311843.5			
B_7		147084.3			
a				0.20	
MAD (%)		8.1	14.9	8.7	11.0
$rms\Delta H^E_m \Delta H^E_m$ J·mol^{-1}		60.9	102.5	62.8	82.2
MaxΔH^E_m /J·mol^{-1}		184.1	258.7	165.3	169.7
Prediction				NRTL	UNIQUAC
22MEE (1) + 1-BuOH (2) + ethanol (3)					
B_0	J·mol^{-1}			0.6746	429.70
B_1				1.3512	283.10
B_2				0.0252	691.99
B_3				0.9577	−100.52
B_4				0.3816	748.65
B_5				−0.2394	−522.17
a_{12}				0.20	
a_{13}				0.20	
a_{23}				0.20	
MAD (%)				17.4	22.2
$rms\Delta H^E_m \Delta H^E_m$ J·mol^{-1}				56.7	102.2
MaxΔH^E_m /J·mol^{-1}				120.1	195.3
22EEE (1) + 1-BuOH (2) + ethanol (3)					
B_0	J·mol^{-1}			0.6746	429.74
B_1				1.3512	283.06
B_2				−0.0879	758.74
B_3				0.7691	−301.87
B_4				0.3816	748.65
B_5				−0.2394	−522.17
a_{12}				0.20	

Table 7 (continued)

Correlation		ΔH^E_{123}, Eq. (12)	ΔH^E_{123}, Eq. (13)	NRTL	UNIQUAC
a_{13}				0.20	
a_{23}				0.20	
MAD (%)				19.57	25.91
$rms\Delta H^E_m$ /J·mol^{-1}				62.1	101.1
MaxΔH^E_m /J·mol^{-1}				148.6	178.4
2ME (1) + 1-BuOH (2) + ethanol (3)					
B_0	J·mol^{-1}			0.6303	274.51
B_1				0.6541	417.49
B_2				0.1009	611.49
B_3				0.4614	−126.54
B_4				0.3816	748.65
B_5				−0.2394	−522.17
a_{12}				0.20	
a_{13}				0.20	
a_{23}				0.20	
MAD (%)				32.4	19.3
$rms\Delta H^E_m$ /J·mol^{-1}				142.4	74.8
Max$\Delta H^E_{m_1}$ /J·mol^{-1}				202.2	159.3
2-PhE (1) + 1-BuOH (2) + ethanol (3)					
B_0	J·mol^{-1}			0.3646	−171.70
B_1				1.1316	1062.23
B_2				−0.0619	134.90
B_3				0.8398	386.41
B_4				0.3816	748.65
B_5				−0.2394	−522.17
a_{12}				0.20	
a_{13}				0.20	
a_{23}				0.20	
MAD (%)				30.1	24.1
$rms\Delta H^E_m$ /J·mol^{-1}				135.7	113.2
Max$\Delta H^E_{m_1}$ /J·mol^{-1}				249.7	275.5

[a]Equivalence between parameters : NRTL $B_0 = t_{12}$; $B_1 = t_{21}$; $B_2 = t_{13}$; $B_3 = t_{31}$; $B_4 = t_{23}$; $B_5 = t_{32}$; UNIQUAC $B_0 = Du_{12}$; $B_1 = Du_{21}$; $B_2 = Du_{13}$; $B_3 = Du_{31}$; $B_4 = Du_{23}$; $B_5 = Du_{32}$

[b]22MEE: 2-(2-MethoxyEthoxy)Ethanol; 22EEE: 2-(2-EthoxyEthoxy)Ethanol; 2ME: 2-Methoxyethanol; 2-PhE : 2-Phenoxyethanol; 1-BuOH: 1-Butanol

Table 8 Summary of the data reduction and prediction results obtained for the studied ternary mixtures: 22MEE. (1) + 1-BuOH (2) + ethanol (3), 22EEE (1) + 1-BuOH (2) + ethanol (3), 2ME (1) + 1-BuOH (2) + ethanol (3) and 2-PhE (1) + 1-BuOH (2) + ethanol (3) at 313.15 K and at $p = 0.1$ MPa. [a,b]

Correlation		H^E_{123}, Eq. (12)	H^E_{123}, Eq. (13)	NRTL	UNIQUAC
22MEE (1) + 1-BuOH (2) + ethanol (3)					
B_0	J·mol^{-1}	17953.7	16459.04	1.3468	858.37
B_1		28418.0	2272.9	0.6700	128.81
B_2		−84061.43	1472.84	1.7509	1884.87
B_3		−211015.3		4.3726	−559.84
B_4		146752.91		102.6979	−466.35
B_5		54589.59		0.1227	761.79
B_6		255520.8			
B_7		−81278.3			
a				0.30	
MAD (%)		7.2	13.5	7.7	8.3
$rms\Delta H^E_m$ /J·mol^{-1}		57.8	93.1	60.5	61.4
MaxΔH^E_m /J·mol^{-1}		156.9	202.9	110.2	138.2
22EEE (1) + 1-BuOH (2) + ethanol (3)					
B_0	J·mol^{-1}	58532.9	30050.62	2.2340	45.59
B_1		−14724.6	−8462.5	3.1411	1220.42
B_2		−240984.09	23760.60	3.1853	8465.71
B_3		−139677.8		1.4699	905.05
B_4		462699.05		−0.5319	225.64
B_5		26728.67		2.0288	−45.69
B_6		229882.7			
B_7		−292845.0			
a				0.30	
MAD (%)		10.71	17.88	6.25	8.31
$rms\Delta H^E_m$J·mol^{-1}		87.7	149.1	56.4	90.9
MaxΔH^E_m /J·mol^{-1}		241.8	443.5	123.7	229.9
2ME (1) + 1-BuOH (2) + ethanol (3)					
B_0	J·mol^{-1}	26597.7	13688.28	1.0558	712.75
B_1		−24050.3	7467.0	0.4911	158.95
B_2		−92533.12	2943.88	1.6280	1762.06
B_3		−92239.0		4.7501	−620.74
B_4		136113.60		102.6980	−319.71
B_5		77997.99		0.1419	545.79
B_6		161951.0			
B_7		−51707.6			
a				0.30	
MAD (%)		6.4	13.1	6.5	7.9

Table 8 (continued)

Correlation		H^E_{123}, Eq. (12)	H^E_{123}, Eq. (13)	NRTL	UNIQUAC
$rms\Delta H^E_m$ J·mol^{-1}		45.0	80.5	45.0	53.8
MaxΔH^E_m /J·mol^{-1}		118.1	171.7	114.0	109.8
2-PhE (1) + 1-BuOH (2) + ethanol (3)					
B_0	J·mol^{-1}	58532.9	30050.62	2.2340	45.59
B_1		−14724.6	−8462.5	3.1411	1220.42
B_2		−240984.09	23760.60	3.1853	8465.71
B_3		−139677.8		1.4699	905.05
B_4		462699.05		−0.5319	225.64
B_5		26728.67		2.0288	−45.69
B_6		311843.5	229882.7	229882.7	
B_7		147084.3	−292845	−292845.0	
a				0.30	
MAD (%)		10.7	17.8	6.2	8.3
$rms\Delta H^E_m$ /J·mol^{-1}		87.7	149.1	56.4	90.9
MaxΔH^E_m /J·mol^{-1}		241.8	443.5	123.7	229.9
Prediction				NRTL	UNIQUAC
22MEE (1) + 1-BuOH (2) + ethanol (3)					
B_0	J·mol^{-1}			0.6470	438.20
B_1				1.3329	298.12
B_2				0.0289	742.50
B_3				0.9492	−117.72
B_4				0.3976	771.39
B_5				−0.2622	−549.02
a_{12}				0.20	
a_{13}				0.20	
a_{23}				0.20	
MAD (%)				22.5 %	24.0 %
$rms\Delta H^E_m$ /J·mol^{-1}				67.6	113.9
MaxΔH^E_m /J·mol^{-1}				131.6	211.1
22EEE (1) + 1-BuOH (2) + ethanol (3)					
B_0	J·mol^{-1}			0.6016	7.88
B_1				1.1842	1014.25
B_2				0.0787	385.57
B_3				0.8380	287.49
B_4				0.3976	771.39
B_5				−0.2622	−549.02
a_{12}				0.20	

Table 8 (continued)

Correlation	H^E_{123}, Eq. (12)	H^E_{123}, Eq. (13)	NRTL	UNIQUAC
a_{13}			0.20	
a_{23}			0.20	
MAD (%)			38.63	29.12
$rms\Delta H^E_m$ /J·mol^{-1}			274.4	206.2
MaxΔH^E_m /J·mol^{-1}			516.1	476.3
2ME (1) + 1-BuOH (2) + ethanol (3)				
B_0	J·mol^{-1}		0.5797	775.12
B_1			0.7865	−117.78
B_2			0.0907	1033.05
B_3			0.4903	−450.24
B_4			0.3976	771.39
B_5			−0.2622	−549.02
a_{12}			0.20	
a_{13}			0.20	
a_{23}			0.20	
MAD (%)			31.4	31.0
$rms\Delta H^E_m$ /J·mol^{-1}			136.1	152.6
MaxΔH^E_m /J·mol^{-1}			190.5	238.6
2-PhE (1) + 1-BuOH (2) + ethanol (3)				
B_0	J·mol^{-1}		0.6016	7.88
B_1			1.1842	1014.25
B_2			0.0787	385.57
B_3			0.8380	287.49
B_4			0.3976	771.39
B_5			−0.2622	−549.02
a_{12}			0.20	
a_{13}			0.20	
a_{23}			0.20	
MAD (%)			38.6	29.1
$rms\Delta H^E_m$ /J·mol^{-1}			274.4	206.2
MaxΔH^E_m /J·mol^{-1}			516.1	476.3

[a]Equivalence between parameters : NRTL $B_0 = t_{12}$; $B_1 = t_{21}$; $B_2 = t_{13}$; $B_3 = t_{31}$; $B_4 = t_{23}$; $B_5 = t_{32}$; UNIQUAC B_0=Du_{12}; B_1=Du_{21}; $B_2 = Du_{13}$; $B_3 = Du_{31}$; $B_4 = Du_{23}$; $B_5 = Du_{32}$

[b]2MEE: 2-(2-MethoxyEthoxy)Ethanol; 22EEE: 2-(2-EthoxyEthoxy)Ethanol; 2ME: 2-Methoxyethanol; 2-PhE : 2-Phenoxyethanol; 1-BuOH: 1-Butanol

Table 9 Modified UNIFAC (Dortmund) group interaction parameters used in this work

Main group		Group interaction parameters		
1	2	a_{12}/K a_{21}/K	b_{12}/K b_{21}/K	c_{12}/K^{-1} c_{21}/K^{-1}
CH_2	OH	2777 1606	−4.674 −4.746	0.001551 0.0009181
CH_2	CH_2O	233.1 −9.654	−0.3155 −0.03242	N/A N/A
CH_2	ACOH	1381 1987	−0.9977 −4.615	N/A N/A
OH	CH_2O	816.7 650.9	−5.092 −0.7132	0.00606 0.000815
OH	ACOH	83.91 465.4	−1.262 −1.841	N/A N/A

Table 10 DM-UNIFAC group decompositions of the compounds investigated in this work

Component	Structure	DM-UNIFAC group decomposition*
2–2(Methoxyethoxy)ethanol	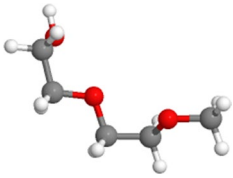	3 CH_2, 1 CH_3O, 1 CH_2O, 1 OH
2–2(Ethoxyethoxy)ethanol	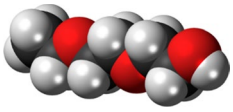	1 CH_3, 3 CH_2, 2 CH_2O, 1 OH
2-Methoxyethanol	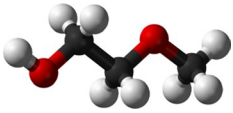	2 CH_2, 1 CH_3O, 1 OH
2-Phenoxyethanol	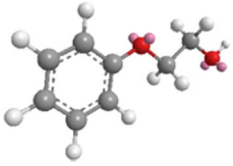	1 ACOH, 2 CH_2, 1 OH
Ethanol		1 CH_3, 1 CH_2, 1 OH
1-Butanol	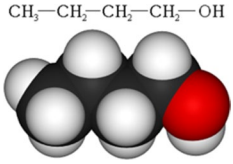	1 CH_3, 3 CH_2, 1 OH

*The decomposition was performed using the Dortmund Data Bank (DDB) and subsequently verified manually according to the group priority rules reported in the original DM-UNIFAC publication [34]

Table 11 Modified UNIFAC (Dortmund) relative Van der Waals volumes R_K and surface areas Q_K [34]

Main group	Subgroup	R_K	Q_K
CH_2	CH_3	0.6325	1.0608
	CH_2	0.6325	0.7081
OH	OH	1.2302	0.8927
CH_2O	CH_3O	1.1434	1.6022
	CH_2O	1.1434	1.2495
	CHO	1.1434	0.8968
ACOH	ACOH	1.080	0.9750

6 Conclusions

To assess their suitability for practical applications, this study emphasizes the role of molecular interactions and structural characteristics in various oxygenated fuel additives. Isothermal H_m^E for the ethanol + 1-BuOH binary blend were experimentally determined at 298.15 K and 313.15 K, under a pressure of 0.1 MPa. Ternary mixtures were then formed by adding one of four glycol ethers to the binary blend: 22MEE, 22EEE, 2ME, and 2-PhE. For each ternary mixture, H_m^E were measured at four different compositions.

All studied mixtures exhibited endothermic behavior at both 298.15 K and 313.15 K under the specified pressure conditions. The experimental data were correlated using the R-K equation, the NRTL model, the Modified UNIFAC (Dortmund) model, and the UNIQUAC model. For the ethanol + 1-BuOH binary blend, the R-K equation showed the closest agreement with the data, yielding AAD values of 0.75% and 1.27% at 298.15 K and 313.15 K, respectively.

For ternary mixtures, the NRTL model was found to be the most accurate in most cases, with AAD values ranging from 5.7% to 8.1%. Experimental data were also predicted using the NRTL, UNIQUAC and UNIFAC models. Across all ternary blends and temperatures, the AAD between experimental and predicted excess molar enthalpy values ranged from 17.4% to 80.4%. The lowest AAD was achieved with the NRTL model, while the highest AAD values were observed with UNIFAC, depending on the specific blend.

These findings demonstrate that the NRTL model provides the most reliable performance for both fitting and predicting the H_m^E of the ternary systems, with predictive errors generally within the range of 17–32%.

Acknowledgements Open access funding provided by UNIVERSIDAD DE BURGOS.

Author Contributions F.E.Y. Writing—Original Draft, Investigation, Software, Formal analysis; K.S.: Writing—Original Draft, Investigation, Software, Formal analysis; M.L. Writing—Review & Editing, Investigation, Software, Supervision, Validation; F.A. Supervision, Validation; F.E.M.A. Supervision, Validation.

Funding Open access funding provided by FEDER European Funds and the Junta de Castilla y León under the Research and Innovation Strategy for Smart Specialization (RIS3) of Castilla y León 2021-2027. No funding was obtained for this study.

Data Availability No datasets were generated or analyzed during the current study.

Declarations

Conflict of interest The authors declare no competing interests.

References

1. W. Sun, *Investigations into the Combustion Kinetics of Several Novel Oxygenated Fuels* (Springer Nature Singapore, Singapore, 2023)
2. S.I. Mohammad, H.A. Owida, A. Vasudevan, S.V. Menon, S. Al-Hasnaawei, S. Ray, N.C. Talniya, A. Sinha, V. Jain, F. Ranjbar, Ind. Crops Prod. **236**, 121916 (2025)
3. M. Anwar, M.G. Rasul, N. Ashwath, Fuel **256**, 115980 (2019)
4. S. Imtenan, H.H. Masjuki, M. Varman, M.A. Kalam, M.I. Arbab, H. Sajjad, S.M.A. Rahman, Energy Convers. Manage. **83**, 149 (2014)
5. J.R.C. Rey, A. Longo, B. Rijo, C.M. Pedrero, L.A.C. Tarelho, P.S.D. Brito, C. Nobre, Fuel **377**, 132776 (2024)
6. H. Kuszewski, Energy Fuels **32**, 11619 (2018)
7. L. Aguado-Deblas, J. Hidalgo-Carrillo, F.M. Bautista, C. Luna, J. Calero, A. Posadillo, A.A. Romero, D. Luna, R. Estévez, Energies **13**, 6584 (2020)
8. S. Ahmad, A.T. Jafry, M.U. Haq, N. Abbas, H. Ajab, A. Hussain, U. Sajjad, Energies **16**, 5153 (2023)
9. A. K. Agarwal and H. Valera, editors , *Potential and Challenges of Low Carbon Fuels for Sustainable Transport* (Springer Singapore, Singapore, 2022).
10. C.J. Orme, J.R. Klaehn, M.K. Harrup, R.P. Lash, F.F. Stewart, J. Appl. Polym. Sci. **97**, 939 (2005)
11. R.D. Chirico, T.W. De Loos, J. Gmehling, A.R.H. Goodwin, S. Gupta, W.M. Haynes, K.N. Marsh, V. Rives, J.D. Olson, C. Spencer, J.F. Brennecke, J.P.M. Trusler, Pure Appl. Chem. **84**, 1785 (2012)
12. X. Zhang, D. Hu, Z. Zhao, J. Chem. Eng. Data **59**, 205 (2014)
13. I. Letyanina, N. Tsvetov, A. Toikka, Fluid Phase Equilib. **405**, 150 (2015)
14. D. Liu, L. Li, R. Lv, Y. Chen, J. Chem. Eng. Data **61**, 2493 (2016)
15. X. Zhang, C. Liu, W. Shen, Y. Ren, D. Li, H. Yang, J. Chem. Thermodyn. **90**, 185 (2015)
16. J.R. Battler, R.L. Rowley, J. Chem. Thermodyn. **17**, 719 (1985)
17. O. Redlich, A.T. Kister, Ind. Eng. Chem. **40**, 345 (1948)
18. M.M. Abbott, H.C. Van Ness, AIChE J. **21**, 62 (1975)
19. D.S. Abrams, J.M. Prausnitz, AIChE J. **21**, 116 (1975)
20. U. Weidlich, J. Gmehling, Ind. Eng. Chem. Res. **26**, 1372 (1987)
21. D. Belhadj, I. Bahadur, A. Negadi, N. Muñoz-Rujas, E. Montero, L. Negadi, J. Chem. Eng. Data **65**, 5192 (2020)
22. I. Mozo, J.A. González, I. García De La Fuente, J.C. Cobos, N. Riesco, J. Mol. Liq. **140**, 87 (2008)
23. R. Francesconi, C. Castellari, F. Comelli, J. Chem. Eng. Data **44**, 1373 (1999)
24. M. De Ruiz Holgado, C. De Schaefer, E.L. Arancibia, J. Chem. Eng. Data **41**, 1429 (1996)
25. P. Reghem, A. Baylaucq, M.J.P. Comuñas, J. Fernández, C. Boned, Fluid Phase Equilib. **236**, 229 (2005)
26. V. Alonso, M. García, J.A. González, I. García De La Fuente, J.C. Cobos, Thermochim. Acta **521**, 107 (2011)
27. V.A. Rana, H.A. Chaube, J. Mol. Liq. **187**, 66 (2013)
28. C. Yang, H. Lai, Z. Liu, P. Ma, J. Chem. Eng. Data **51**, 1345 (2006)

29. C. Vallés, E. Pérez, M. Cardoso, M. Domínguez, A.M. Mainar, J. Chem. Eng. Data **49**, 1460 (2004)
30. S. Murakami, G.C. Benson, J. Chem. Thermodyn. **1**, 559 (1969)
31. F. Aguilar, F.E.M. Alaoui, C. Alonso-Tristán, J.J. Segovia, M.A. Villamañán, E.A. Montero, J. Chem. Eng. Data **54**, 1672 (2009)
32. P. Reference, Expr. Uncertain. Meas. Calibration 20 (1999).
33. P. Bevington and D. Robinson (2003) Data Reduct. Error Anal. Phys. Sci. 194.
34. J. Gmehling, J. Li, M. Schiller, Ind. Eng. Chem. Res. **32**, 178 (1993)
35. M. Lifi, I. Abala, N. Munoz-Rujas, F. Aguilar, E.A. Montero, L. Negadi, F.E. M'hamdi Alaoui, J. Chem. Thermodyn. **164**, 106593 (2022)
36. H. Lifi, R. Aitbelale, M. Lifi, N. Muñoz-Rujas, F. Ezzahrae M'hamdi. Alaoui, F. Aguilar, J. Chem. Thermodyn. **201**, 107406 (2025)
37. M. Lifi, I. Abala, R. Briones-Llorente, N. Muñoz-Rujas, F. Aguilar, F.E. M'hamdi Alaoui, J. Chem. Eng. Data **68**, 3062 (2023)
38. A.E. Pope, H.D. PFlug, B. Dacre, G.C. Benson, Can. J. Chem. **45**, 2665 (1967)
39. C. Medcraft, S. Zinn, M. Schnell, A. Poblotzki, J. Altnöder, M. Heger, M.A. Suhm, D. Bernhard, A. Stamm, F. Dietrich, M. Gerhards, Phys. Chem. Chem. Phys. **18**, 25975 (2016)